Figure 3. Disease-specific Kaplan-Meier survival curves of 45 patients stratified by livin expression in RCC tissues **(A)** and serum anti-livin antibodies **(B)**.

We also demonstrated that 56% of RCC patients had high anti-livin autoantibody titer in their sera. There was a significant relationship between livin expression in RCC tissues and the titer of the anti-livin Ab, but the survival of patients with high anti-livin Ab titers was not different from that of patients with low titers. Moreover, 7 patients (16%) had low anti-livin Ab titers although their RCC tissues expressed livin. Those results suggest that the amount of the anti-livin Ab produced during the natural history of RCC did not reflect antitumor responses. However, Schmollinger et al.[4] reported that vaccination with irradiated autologous melanoma cells engineered to secrete granulocyte macrophage colony-stimulating factor by retrovirus-mediated gene transfer induced anti-livin Abs, and the reactions were associated with cellular immune responses, including livin-specific CD4+ and CD8+ T cells. We plan to evaluate livin-specific cellular immune reactions in RCC patients and start a clinical trial of vaccination targeting livin, evaluating the relationship between the anti-livin Ab titer and the cellular immune and clinical responses. Furthermore, it would be interesting to evaluate whether RCC patients with high anti-livin Ab titers show good responses to immunotherapies.

There were 6 patients (13%) with the anti-livin Ab in serum despite having score 0 for livin expression in the RCC tissue. It is possible that less than 10% of livin-positive cells might affect the immune system in patients because livin is not expressed in normal tissues.[1,3,5] It is also speculated that livin-positive RCC cells might be rejected immunologically in the early phase of progression and that only livin-negative ones might remain and progress in such patients. In any case there was no healthy volunteer with a high anti-livin Ab titer. Therefore, it seems that tumor-expressed livin can be recognized by the host immune system in patients with high anti-livin Ab titers.

CONCLUSIONS

We have demonstrated that livin is expressed in approximately 60% of RCC cases. Livin expression may not provide predictive information, but the anti-livin Ab titer in the sera of RCC patients was significantly higher than that in healthy volunteers. Although the immune responses without immunotherapeutic stimulation did not affect patient survival, livin may be recognized as a tumor antigen by the immune system in RCC patients. These findings provide a rationale for further evaluation of immune responses by a tumor vaccine targeting livin.

References

1. Kasof GM, and Gomes BC: Livin, a novel inhibitor of apoptosis protein family member. J Biol Chem **276**: 3238–3246, 2001.
2. Hussein MR, Haemel AK, and Wood GS: Apoptosis and melanoma: molecular mechanisms. J Pathol **199**: 275–288, 2003.
3. Lin JH, Deng G, Huang Q, et al: KIAP, a novel member of the inhibitor of apoptosis protein family. Biochem Biophys Res Commun **279**: 820–831, 2000.
4. Schmollinger JC, Vonderheide RH, Hoar KM, et al: Melanoma inhibitor of apoptosis protein (ML-IAP) is a target for immune-mediated tumor destruction. Proc Natl Acad Sci U S A **100**: 3398–3403, 2003.
5. Hariu H, Hirohashi Y, Torigoe T, et al: Aberrant expression and potency as a cancer immunotherapy target of inhibitor of apoptosis protein family, Livin/ML-IAP in lung cancer. Clin Cancer Res **11**: 1000–1009, 2005.
6. Ashhab Y, Alian A, Polliack A, et al: Two splicing variants of a new inhibitor of apoptosis gene with different biological properties and tissue distribution pattern. FEBS Lett **495**: 56–60, 2000.
7. Altieri DC: The molecular basis and potential role of survivin in cancer diagnosis and therapy. Trends Mol Med **7**: 542–547, 2001.
8. Mahotka C, Krieg T, Krieg A, et al: Distinct in vivo expression patterns of survivin splice variants in renal cell carcinomas. Int J Cancer **100**: 30–36, 2002.
9. Shariat SF, Lotan Y, Saboorian H, et al: Survivin expression is associated with features of biologically aggressive prostate carcinoma. Cancer **100**: 751–757, 2004.
10. Yagihashi A, Asanuma K, Tsuji N, et al: Detection of anti-livin antibody in gastrointestinal cancer patients. Clin Chem **49**: 1206–1208, 2003.
11. Parker AS, Kosari F, Lohse CM, et al: High expression levels of survivin protein independently predict a poor outcome for patients who undergo surgery for clear cell renal cell carcinoma. Cancer **107**: 37–45, 2006.

Efficient Cross-Presentation by Heat Shock Protein 90-Peptide Complex-Loaded Dendritic Cells via an Endosomal Pathway

Takehiro Kurotaki,*[†] Yasuaki Tamura,[1]* Gosei Ueda,*[‡] Jun Oura,* Goro Kutomi,*
Yoshihiko Hirohashi,* Hiroeki Sahara,* Toshihiko Torigoe,* Hiroyoshi Hiratsuka,[‡]
Hajime Sunakawa,[‡] Koichi Hirata,[†] and Noriyuki Sato*

It is well-established that heat shock proteins (HSPs)-peptides complexes elicit antitumor responses in prophylactic and therapeutic immunization protocols. HSPs such as gp96 and Hsp70 have been demonstrated to undergo receptor-mediated uptake by APCs with subsequent representation of the HSP-associated peptides to MHC class I molecules on APCs, facilitating efficient cross-presentation. On the contrary, despite its abundant expression among HSPs in the cytosol, the role of Hsp90 for the cross-presentation remains unknown. We show here that exogenous Hsp90-peptide complexes can gain access to the MHC class I presentation pathway and cause cross-presentation by bone marrow-derived dendritic cells. Interestingly, this presentation is TAP independent, and followed chloroquine, leupeptin-sensitive, as well as cathepsin S-dependent endosomal pathways. In addition, we show that Hsp90-chaperoned precursor peptides are processed and transferred onto MHC class I molecules in the endosomal compartment. Furthermore, we demonstrate that immunization with Hsp90-peptide complexes induce Ag-specific CD8+ T cell responses and strong antitumor immunity in vivo. These findings have significant implications for the design of T cell-based cancer immunotherapy. *The Journal of Immunology*, 2007, 179: 1803–1813.

Heat shock proteins (HSPs)[2] are molecular chaperones that control the folding and prevent the aggregation of proteins. Recent studies have demonstrated that tumor-derived HSP, such as Hsp70, Hsp90, and gp96, initiate tumor-specific CTL responses and protective immunity (1). In this process, APCs internalize exogenously administered HSP with bound peptides by receptor-mediated endocytosis, resulting in Ag presentation via MHC class I molecules (2–5). Indeed, though a number of cellular receptors for HSPs have been described, including CD91 (6), CD40 (7), TLR2/4 (8), LOX-1 (9), and SR-A (10), as receptors for several kinds of HSPs (11), it is not clear which receptors are responsible for uptake and/or proinflammatory signaling. Tumor-bearing mice immunized with Hsp70 or gp96 isolated from the tumors or complexes of Hsp70 or gp96 reconstituted in vitro with known peptide Ags have been shown to mount a potent CD8+ T cell response that can reduce or eliminate tumor progression (12–14).

In contrast, dendritic cells (DCs) have the capacity to take up, process, and present exogenous Ags in association with MHC class I molecules. This process is termed cross-presentation and the resulting CD8+ T cell priming is referred to as cross-priming. It has been demonstrated that some exogenous Ags such as HSPs and particulated protein Ags gain access to the MHC class I-processing pathway and initiate CTL responses (1). This exogenous pathway is important for the development of CD8+ CTL responses against tumors and infectious pathogens that do not have access to the classical MHC class I pathway. Administration of antigenic peptides in the context of purified HSPs induces potent CD8+ T cell responses, indicating that HSP-peptide complexes can access the MHC class I endogenous Ag-presentation pathway (2, 13, 15–19). Thus, shuttling exogenous peptides into the endogenous pathway might be a specialized function of HSPs. However, the precise mechanism of HSP-mediated cross-presentation remains to be elucidated.

Considering the significance of HSP-mediated cross-presentation in vivo, the release of tumor cell contents, presumably including HSPs, and their uptake by APC would occur when tumor cells die either naturally, as a result of hypoxia, or because of therapeutic intervention (20–22). Given the important role of HSPs as a "danger signal," proposed by Matzinger and colleague (23), HSPs released into the extracellular milieu may act simultaneously as an Ag source due to their ability to chaperone peptides and as a maturation signal for dendritic cells, thereby inducing DCs to cross-present Ags to CD8+ T cells.

Hsp90 is one of the most abundant proteins within cells and is overexpressed in many cancer cells. Therefore, once cancer cells become necrotic, much Hsp90 would be released from cells and might act as a danger signal, subsequently eliciting cell-specific immune responses. It has been demonstrated that the tumor-derived Hsp90-peptide complex elicits tumor-specific immunity (24). Moreover, Kunisawa and Shastri (25) have recently shown that cells generate large, C-terminally extended proteolytic intermediates that are associated with Hsp90. In this context, cell-derived Hsp90-C-terminally extended precursor peptide complexes could be released into the extracellular milieu, followed by uptake by APCs, when tumor cells are exposed to stress. At

present, however, the Ag-processing pathway yielding the transfer of exogenous Hsp90-associated peptide Ags to MHC class I molecules is unknown.

In this study, we examined the roles of Hsp90 in MHC class I-restricted cross-presentation using bone marrow-derived DC (BMDC) as APCs. We show that Hsp90-peptide complexes reconstituted in vitro enter the endosomal pathways, which are chloroquine-, leupeptin-, and cathepsin S-sensitive. Furthermore, we show that chaperoned peptides are loaded onto endosomal (recycling) MHC class I molecules in the early endosome. Intriguingly, this presentation occurs within 30 min, indicating that very rapid and efficient processing might be achieved within BMDC. Moreover, we show that immunization with Hsp90-peptide complexes elicits very strong peptide-specific CTLs in vivo as well as therapeutic effects. Thus, we propose that Hsp90 acts as an excellent guide for cross-presentation of chaperoned Ags. Our data provide novel insights into the role of extracellular Hsp90-peptide complexes in cross-priming and peptide-based cancer immunotherapy.

Materials and Methods

Mice

C57BL/6 (H-2^b), B6C3F1 (H-2$^{b/k}$), and TAP1$^{-/-}$ mice were obtained from The Jackson Laboratory. HLA-A*2402/K^b transgenic mice were purchased from SLC Japan. All mice were kept in a specific pathogen-free mouse facility. Studies were performed according to institutional guidelines for animal use and care.

Cells

The mouse thymoma cell line EL4 and its E.G7 derivative (EL4 transfected with cDNA encoding OVA) were obtained from American Type Culture Collection (ATCC). N1 is an EL4 cell transfected with the nucleocapsid gene of vesicular stomatitis virus (VSV). An established CTL clone specific for the VSV8 epitope in the context of H-2K^b was restimulated with N1 every 7 days. The B3Z cell is a CD8$^+$ T cell hybridoma specific for the OVA$_{258-265}$ epitope (SL8) in the context of H-2K^b. The KZO cell is a CD4$^+$ T cell hybridoma specific for the OVA$_{247-265}$ (PL19) in the context of I-A^k. These hybridomas were a gift from Dr. N. Shastri (University of California, Berkeley, CA). RMA-S-A*2402 cells were RMA-S transfected with the gene encoding HLA-A*2402 (provided by Dr. H. Takasu, Dainippon-Sumitomo Pharmaceutical, Osaka, Japan). TG-3 cells are a methylcholanthrene-induced fibrosarcoma derived from the HLA-A*2402 transgenic mouse. TG-3-2B cells were TG-3 transfected with the gene encoding human survivin-2B. Survivin-2B$_{80-88}$-specific CTLs were restimulated with survivin-2B$_{80-88}$ peptide-pulsed splenocytes every 7 days. BMDC were generated from the femurs and tibiae of C57BL/6 or HLA-A*2402/K^b transgenic mice. The bone marrow was flushed out, and the leukocytes were obtained and cultured in complete RPMI 1640 with 10% heat-inactivated FCS and 20 ng/ml GM-CSF (Endogen) for 5 days. On day 3, fresh medium with GM-CSF was added to the plates for the day 5 cultures.

Plasmid construction

FLAG-tagged human survivin-2B cDNA was amplified from HeLa cells by RT-PCR method and constructed in the plasmid pCDNA3.1$^+$ (Invitrogen Life Technologies). Primer pairs used for RT-PCR were 5'-CGGGAT CCATGGGTGCCCCGACGTTGCCC-3' and 5'-CCGCTCGAGATCCA TGGCAGCCAGCTGCTC-3' as forward and reverse primers, containing BamHI and XhoI sites, respectively. The purified PCR product was digested with BamHI and XhoI restriction enzymes, then ligated into digested pCDNA3.1$^+$ plasmid. The sequence of the cDNA was confirmed with ABI Genetic analyzer PRIM 3100 (PerkinElmer).

Proteins and Abs

Purified human Hsp90 and recombinant human Hsp72 were purchased from StressGen Biotechnologies. Chicken OVA was purchased from Calbiochem. BSA, fucoidin, and α2 macroglobulin (α2M) were obtained from Sigma-Aldrich. mAbs anti-H-2K^b (clone AF6-88.5), anti-H-2D^b (clone 28-14-8), and anti-HLA-DR (L243) were purchased from BD Pharmingen. mAb anti-MHC class I (W6/32) was purchased from ATCC. mAb anti-HLA-A24 (C7709A2.6) was provided by Dr. P. G. Coulie (Christian de

Duve Institute of Cellular Pathology, University of Louvain, Brussels, Belgium). mAb anti-HLA-A31 was established in our laboratory. Organelles were detected by confocal laser microscopy with specific Abs against KDEL (clone 10C3; StressGen Technologies) for ER, Rho B (Santa Cruz Biotechnology) for endosomes, and CD107a (LAMP-1) (clone 1D4B; BD Pharmingen) for lysosomes. Each Ab was labeled with Alexa Fluor 594 (Molecular Probes). mAb 25D1.16 specific for the K^b/OVA$_{257-264}$ complexes was provided by Dr. R. Germain (National Institutes of Health, Bethesda, MD). Anti-mouse CD16/CD32 Fc-block was purchased from BD Pharmingen.

Generation of Hsp90-peptide/protein complex in vitro

The following peptides were used (underlined sequences represent the precise MHC class I-binding epitope): survivin-2B$_{80-88}$ peptide (AYACNT STL), survivin-2B$_{75-93}$ (GPGTVAYACNTSTLGGRGG) VSV 8 (RGYV YQGL), VSV-C (RGYVYQGLKSGNVSC), SL8 (SIINFEKL), and SL8C (SIINFEKLTEWTS). In vitro reconstitution was conducted as previously described (13). Hsp90 was mixed with a ^{125}I-labeled peptide in a 50:1 peptide to a protein molar ratio in 0.7 M NaCl containing sodium-phosphate buffer and heated at 45°C for 10 min then incubated at room temperature for 30 min. Hsp90 (10 μg) and OVA (10 μg) were mixed and incubated for 10 min at 45°C. The samples were then incubated for 30 min at room temperature. Free OVA was removed completely using a Microcon YM-100 (Millipore). In the case of Hsp72, peptides and Hsp72 were co-incubated at 37°C in sodium phosphate buffer containing 1 mM ADP and 1 mM MgCl$_2$. Samples were analyzed by SDS-PAGE and staining, followed by autoradiography of the stained gel.

Vaccination and induction of CTL

Each HLA-A*2402/K^b transgenic mouse was immunized s.c. at the base of the tail four times at 1-wk intervals, with Hsp90 (50 μg) alone, the Hsp90 (50 μg)-survivin-2B$_{80-88}$ peptide (AYACNTSTL) (50 μg) complex, survivin-2B$_{80-88}$ peptide (50 μg) with IFA or CFA individually. One week after the last immunization, spleen cells were removed, cultured in vitro with irradiated (100 Gy) and survivin-2B$_{80-88}$ peptide-pulsed spleen cells for 5 days. Subsequently, the generation of survivin-2B$_{80-88}$ peptide-specific CTLs was evaluated in a ^{51}Cr-release assay. The specificity of CTLs induced in an individual HLA-A*2402/K^b transgenic mouse was evaluated using RMA-S/A*2402 cells as targets in the presence or absence of the survivin-2B$_{80-88}$ peptide.

^{51}Cr-release assay

The cytolytic activity of the induced CTL was determined by a standard 4 h-^{51}Cr-release assay described earlier (19). To determine the MHC class I restriction in the cytotoxic assay, indicated amount of mAbs against HLA class I (W6/32), HLA-A24, HLA-A31, and HLA class II (L231) were added to each well. In the case of VSV or OVA system, 10 μg/ml mAbs against H-2K^b and H-2D^b were added to the each well.

Transplantation of tumor cells and immunotherapy

TG3-2B cells (5 × 10^5) were intradermally transplanted into the right flank in HLA-A*2402/K^b transgenic mice on day 0. When average tumor diameter reached 5 mm, the mice were then treated with Hsp90 (50 μg) alone, the Hsp90 (50 μg)-survivin-2B$_{80-88}$ peptide (50 μg) complex, or survivin-2B$_{80-88}$ peptide (50 μg) emulsified in IFA via s.c. administration at the nape of the neck twice each week for 2 wk (on days 9, 13, 16, and 20). Control groups of mice were immunized with PBS. Tumor growth was recorded twice each week. Average diameters of the two axes were plotted so that therapeutic effects could be compared among the groups. Average tumor diameters on day 29 were statistically analyzed using the Mann-Whitney U test. In addition, mouse survival was monitored every other day. Statistical analyses for evaluating the survival advantages were performed using log-rank analysis. All the experiments were performed with 10 mice/group.

ELISPOT assay

The specificity of CTLs for the survivin-2B$_{80-88}$ peptide was also evaluated by IFN-γ ELISPOT assay. Splenic CD8$^+$ T cells were isolated from mice immunized with Hsp90-survivin-2B$_{80-88}$ peptide, which were cultured for 5 days described above, with MACS (Miltenyi Biotec) using an anti-mouse CD8a mAb coupled with magnetic microbeads according to the manufacturer's instructions. As target cells, RMA-S/A*2402 cells were cultured overnight at 26°C in RPMI 1640 supplemented with 10% FBS, 2.5 μg/ml β$_2$-microglobulin, 100 μg/ml survivin-2B$_{80-88}$ peptide, an irrelevant CMV peptide (QYDPVAALF), or without any peptide. Ninety-six-well ELISPOT plates (BD Biosciences) were coated with 5.0 μg/ml rat

anti-mouse IFN-γ mAb and subsequently blocked with RPMI 1640 supplemented with 10% FBS for 2 h at room temperature. Then, 5×10^3 CTLs and 1×10^5 each target cells were added to the wells and cultured for 12 h at 37°C in RPMI 1640 in 10% FBS. The plates were then washed extensively and incubated with a 2.0 μg/ml biotinylated anti-mouse IFN-γ mAb, followed by pulsing with 0.5 μg/ml streptavidin-HRP. Positive spots were developed by adding 100 μl/well AEC Substrate Solution (BD Biosciences) and were counted using a Vision ELISPOT reader (Carl Zeiss).

Production of retrovirus and virus infection

The HLA-A*2402 cDNA was inserted into BamHI and NotI sites of the pMXs-puro retrovirus expression vector (26) (gift from Prof. T. Kitamura, University of Tokyo, Tokyo, Japan). High-titer retrovirus carrying HLA-A*2402 was produced in a transient retrovirus-packaging cell line PLAT-E (27) (gift from Prof. T. Kitamura). Briefly, PLAT-E cells were transfected with 5 μg of retrovirus vector plasmid with the FuGene HD Transfection Reagent (Roche Molecular Diagnostics). At 48 h after transfection, the supernatant was harvested as viral stock solution. For infection, immature BMDCs from TAP$^{-/-}$ mice were incubated for 6 h with 6 ml of virus stock solution in the presence of 8 μg/ml hexadimethrine bromide (Sigma-Aldrich). Twenty-four hours postinfection, the mouse BMDCs were used for assays. The expression of HLA-A24 was confirmed by flow cytometry using an anti-HLA-A24 mAb (C7709A2.6) and 20–30% of DCs were HLA-A24 positive.

In vitro cross-presentation assay

Immature BMDCs (1×10^4) from HLA-A*2402/K^b transgenic mice or HLA-A*2402-transduced BMDCs (1×10^4) derived from TAP$^{-/-}$ mice were pulsed with an Hsp90 (10 μg/ml)-survivin-2B$_{75-93}$ precursor peptide (100 ng/ml) complex generated in vitro, Hsp90 alone (10 μg/ml), survivin-2B$_{80-88}$ peptide (100 ng/ml), or survivin-2B$_{75-93}$ precursor peptide (100 ng/ml), and survivin-2B$_{80-88}$-specific CTLs (1×10^5) were added to the cultures. In VSV or OVA system, immature BMDCs (1×10^4) from C57BL/6 and TAP$^{-/-}$ mice were pulsed with an Hsp90 (10 μg/ml)-peptide (10 μg/ml) or OVA protein (10 μg/ml) complex generated in vitro, and peptide-specific CTLs (1×10^5) were added to the cultures. The assay was conducted in 200-μl volume in 96-well plates with AIM-V (Invitrogen Life Technologies) at 37°C for 20 h. Culture supernatants were harvested and tested for the presence of IFN-γ release by ELISA (Cytimmune Sciences). In the case of OVA system, SL8/K^b-specific B3Z or PL19/A^k-specific KZO responses were measured as the β-galactosidase activity induced upon ligand recognition. The B3Z (1×10^5) or KZO (1×10^5) and Ag-loaded BMDCs (5×10^4) were added to each well and cultured overnight. The β-galactosidase activity was measured at the absorbance at 595 nm of the cleavage product of chlorophenol red β-pyranoside.

Immunocytological localization of exogenous Hsp90

Hsp90 was conjugated with Alexa Fluor 488 (Molecular Probes) according to the manufacturer's instructions. Immature BMDCs were pulsed with the Alexa Fluor 488-labeled Hsp90 (20 μg/ml)-SL8C peptide (20 μg/ml) complex for 2 h. After incubation, cells were fixed with ice-cold acetone for 1 min, and then stained with an anti-Rho B Ab for detecting early endosomes, anti-KDEL mAb for ER, and anti-LAMP1 for late endosomes and lysosomes followed by Alexa Fluor 594-conjugated goat anti-rabbit IgG or anti-mouse IgG and visualized using a Bio-Rad MRC1024ES laser confocal scanning microscopy system (Bio-Rad). For detecting the intracellular localization of recycling MHC class I molecules and SL8-K^b complexes, the DCs were incubated with anti-mouse CD16/CD32 Fc-block to block nonspecific staining, and then costained with an Alexa Fluor 488-labeled Hsp90-SL8C peptide complex and Alexa Fluor 594-labeled anti-H-2K^b mAb (clone AF6-88.5) or Alexa Fluor 488-labeled 25D1.16 mAb and anti-organelle Abs conjugated with Alexa Fluor 594 and visualized by confocal laser microscopy.

Detection of fluorescent Hsp90-peptide complexes association with BMDCs and competition assay

BMDCs (1×10^5) were preincubated with Hsp90, BSA, human α2M (Sigma-Aldrich), or fucoidin (Sigma-Aldrich) at indicated concentrations (25, 50, 100 μg) for 10 min at 4°C, then pulsed with the Alexa Fluor 488-labeled Hsp90 (5 μg)-SL8 peptide (10 μg) complex for 10 min at 4°C. The BMDCs were then washed twice with ice-cold PBS, fixed with ice-cold acetone for 1 min, and analyzed by flow cytometry and confocal laser microscopy.

Inhibition studies

For most inhibition studies, immature BMDCs (10^5 cells/well) were first incubated in 0.1 ml of each drug for 2 h. Then Hsp90 (10 μg/ml)-SL8C (10 μg/ml) complex, SL8C (10 μg/ml) or OVA protein (40 μg/ml) of Ag was added to the wells (0.2 ml final volume) at the final concentration indicated in the continuous presence of inhibitors for 2 h. BMDCs were then washed three times and fixed with 0.05% glutaraldehyde (Sigma-Aldrich). Fixation was stopped by addition of 2 M L-lysine (Sigma-Aldrich) and cells were washed twice in PBS. Thereafter, SL8/K^b-specific B3Z or PL19/A^k-specific KZO were added to each well and cultured overnight. The β-galactosidase activity was measured at the absorbance at 595 nm. The inhibitors used were primaquine, chloroquine, lactacystin, leupeptin, and pepstatin (all obtained from Sigma-Aldrich except for primaquine (ICN Biomedicals)). LLnL, cathepsin S inhibitor (Z-FL-COCHO), cathepsin B inhibitor (Ac-Leu-Val-lysinal), and cathepsin L inhibitor (Z-FF-FMK) were purchased from Merck Biosciences.

Results

Efficient induction of tumor peptide-specific CTL by immunizing Hsp90-peptide complex

We previously reported that survivin and its splicing variant survivin-2B are expressed abundantly in various types of tumor tissues and are suitable as target Ags for tumor immunotherapy. Subsequently, we identified an HLA-A24-restricted antigenic peptide, survivin-2B$_{80-88}$ (AYACNTSTL) recognized by CD8$^+$ CTLs (28, 29). On the basis of these observations, we have started a phase I clinical study of survivin-2B$_{80-88}$ peptide vaccination for patients with advanced colorectal cancer. To establish an effective cancer vaccine, the development of an effective and safe adjuvant remains a high priority. Therefore, we examined whether HSPs could be a good candidate for a cancer vaccine adjuvant. First, we confirmed that the two major HSPs, Hsp70 and Hsp90, but not the control protein transferrin, were made complexed with survivin-2B$_{80-88}$ peptides in vitro (Fig. 1A). Next, we tested the ability of Hsp70 and Hsp90 to generate CTL responses against associated peptides. HLA-A*2402/K^b transgenic mice are a well-established model for studying HLA-A*2402-restricted CTL epitopes and vaccine development (30). These mice contain transgenic chimeric human α1 and α2 domains of HLA-A*2402 and mouse α3 transmembrane and cytoplasmic domains of H-2K^b, which increase the level of T cell responsiveness. We immunized these transgenic mice with the Hsp70-survivin-2B$_{80-88}$ peptide complex or Hsp90-survivin-2B$_{80-88}$ peptide complex and examined the induction of peptide-specific CTL responses. As shown in Fig. 1B, spleen cells of mice immunized with the Hsp90-survivin-2B$_{80-88}$ peptide complex showed significant cytotoxicity against survivin-2B$_{80-88}$-coated RMA-S-A*2402 cells, but not survivin-2B$_{80-88}$-noncoated RMA-S-A*2402 cells. This cytotoxic activity was almost same as from mice immunized with survivin-2B$_{80-88}$ emulsified in CFA (Fig. 1G). In contrast, spleen cells of mice immunized with the Hsp70-survivin-2B$_{80-88}$ peptide complex (Fig. 1D), Hsp90 alone (Fig. 1C), Hsp70 alone (Fig. 1E) or survivin-2B emulsified in IFA (Fig. 1F) did not show much cytotoxicity against survivin-2B$_{80-88}$-coated RMA-S-A*2402. This cytotoxicity was significantly blocked by pretreatment of target cells with an anti-human MHC class I mAb W6/32 and an anti HLA-A24 mAb, but not with an anti-HLA-A31 mAb (Fig. 1H). Similarly, pretreatment of effector cells with anti-CD8, but not with anti-CD4 mAb, significantly blocked the cytotoxicity against survivin-2B$_{80-88}$-coated RMA-S-A*2402 cells (data not shown). Furthermore, to determine whether this cytotoxic function was related to the frequency of peptide-specific T cells, ELISPOT assay was performed using splenocytes from each immunized mouse. Purified CD8$^+$ T cells from splenocytes after 5 days in vitro stimulated with survivin-2B$_{80-88}$ were cocultured for 12 h with RMA-S/A*2402 cells alone, RMA-S/A*2402 pulsed with survivin-2B$_{80-88}$, or those pulsed with an

FIGURE 2. Immunization with Hsp90-Ag peptide complex generated CTLs recognizing chaperoned peptide. Purified splenic CD8^{+} T cells from Hsp90-survivin-2B$_{80-88}$ peptide-immunized mice were stimulated with the survivin-2B$_{80-88}$ peptide in vitro. Responding CTLs were tested for IFN-γ ELISPOTs in response to RMA-S/A*2402 cells without peptide pulsing, pulsed with an irrelevant CMV peptide, or pulsed with the survivin-2B$_{80-88}$ peptide. The number of ELISPOTs produced by 5×10^3 CTLs in response to 1×10^5 RMA-S/A*2402 cells is shown.
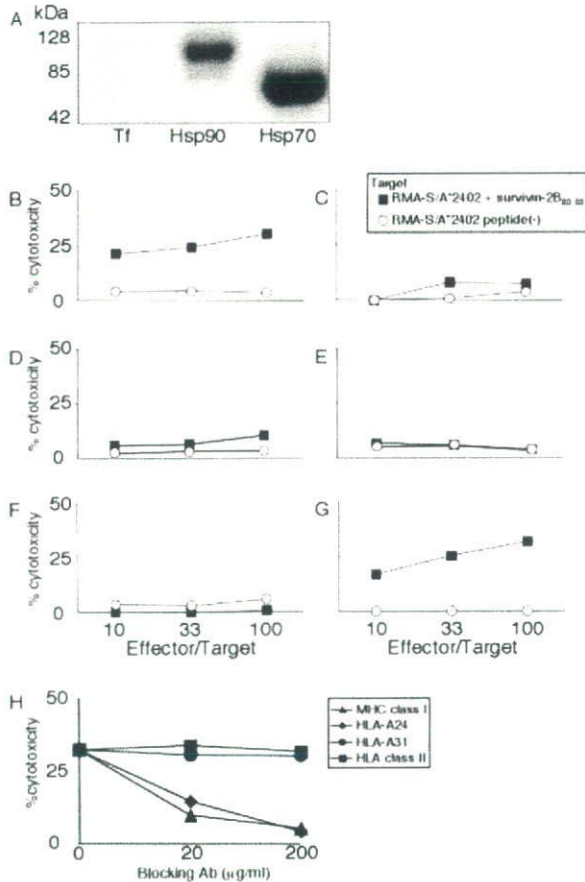
FIGURE 1. Efficient induction of peptide-specific CTL response in mice vaccinated with Hsp90-peptide complexes. *A*, Hsp90, Hsp70, and transferrin (Tf) were mixed with a ^{125}I-labeled peptide in a 50:1 peptide protein ratio in sodium-phosphate buffer. Samples were analyzed by SDS-PAGE and staining (data not shown), followed by autoradiography of the stained gel. Hsp90 and Hsp70 bound the survivin-2B$_{80-88}$ peptide efficiently, but not transferrin. *B–G*, HLA-A*2402/K^b-transgenic mice were immunized s.c. four times with the Hsp90-survivin-2B$_{80-88}$ peptide complex (*B*), Hsp90 alone (*C*), Hsp70-survivin-2B$_{80-88}$ peptide complex (*D*), Hsp70 alone (*E*), and survivin-2B$_{80-88}$ peptide emulsified with IFA (*F*) or CFA (*G*) individually. Spleen cells were removed 1 wk after the last immunization, cultured for 5 days with survivin-2B$_{80-88}$ peptides, and tested for cytotoxicity. Each line represents the specific lysis of target cells by spleen cells from one individual mouse. Target cells were RMA-S/A*2402 cells pulsed with the survivin-2B$_{80-88}$ peptide (■) or without the peptide (□). *H*, Peptide-specific cytotoxicity was induced in MHC class I-restricted fashion. Indicated amount of mAbs against HLA class I (W6/32), HLA-A24 (C7709A2.6), HLA-A31, and HLA class II (L231) were added to each well.

irrelevant CMVpp65-derived peptide (QYDPVAALF). The number of IFN-γ ELISPOTs produced by 5×10^3 CD8^{+} T cells against 1×10^5 RMA-S/A*2402 cells are shown in Fig. 2. CD8^{+} T cells efficiently produced IFN-γ ELISPOTs in response to RMA-S/*A2402 cells pulsed with survivin-2B$_{80-88}$ peptide, but not in response to RMA-S/A*2402 cells alone or RMA-S*A2402 cells pulsed with the irrelevant CMVpp65-derived peptide (QYDPVAALF). These findings confirmed the fact that the CTLs were specific for survivin2B$_{80-88}$. Thus, we demonstrated that Hsp90 was a fairly good adjuvant for a T cell-mediated antitumor vaccine.

Cross-presentation of Hsp90-chaperoned peptide in the context of MHC class I by BMDCs

Next, we tested whether in vitro reconstituted Hsp90-peptide complexes were taken up and associated peptides were presented in the
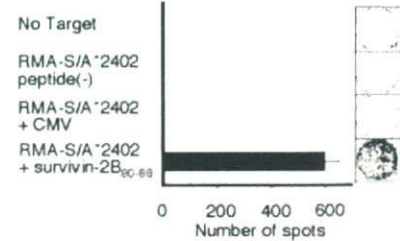
context of MHC class I molecules by BMDCs. To monitor the MHC class I Ag-processing pathway, we used Hsp90 reconstituted in vitro with a precursor peptide of survivin2B$_{80-88}$, survivin-2B$_{75-93}$ (19 mer). The Hsp90-survivin-2B$_{75-93}$ precursor peptide complex was cocultured with BMDCs for 2 h and fixed, followed by incubation with a survivin-2B$_{80-88}$-specific CTL clone. The culture supernatant was assayed for the production of IFN-γ. As shown in Fig. 3, the Hsp90-survivin-2B$_{75-93}$ precursor peptide complex was processed and presented by HLA-A*2402, and consequently recognized by the survivin-2B$_{80-88}$-specific CTL clone but not Hsp90 or the survivin-2B$_{75-93}$ precursor peptide alone. This phenomenon was also observed by the standard ^{51}Cr-release assay (data not shown). These data suggested that the Hsp90-chaperoned precursor peptide was processed to an epitope within the cells with subsequent access to the MHC class I pathway, a process known as cross-presentation.

Vaccination of mice with Hsp90-peptide complex promotes antitumor effect

We then examined the efficacy of the Hsp90-based immunotherapy using the human tumor Ag survivin-2B as a surrogate Ag. To assess whether cross-presentation of the Hsp90-survivin-2B$_{80-88}$ complexes elicits antitumor effects in vivo, we developed TG3 with surrogate Ag human survivin-2B, TG3-2B. Although, the TG3-2B cell line is an artificial tumor model, we thought that it was necessary to examine whether the in vitro cross-presentation
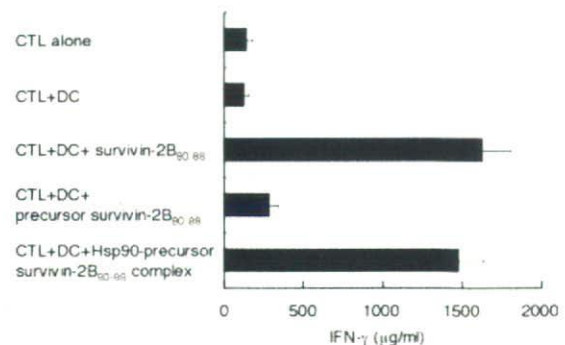
FIGURE 3. Cross-presentation of Hsp90-chaperoned peptide by BMDCs. Survivin-2B$_{80-88}$, precursor survivin-2B$_{80-88}$ (19 mer), or Hsp90-precursor survivin-2B$_{80-88}$ complex was loaded to HLA-A*2402/K^b-transgenic mouse-derived BMDCs for 2 h and a survivin-2B$_{80-88}$-specific CTL clone was added. IFN-γ in the culture supernatant was measured by ELISA.
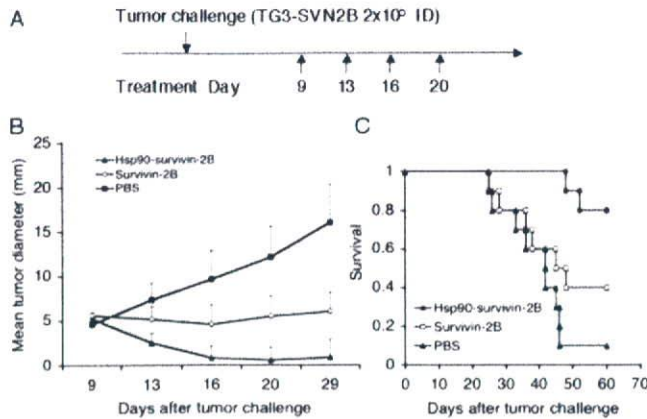
FIGURE 4. Hsp90-tumor Ag peptide complex induces strong antitumor effect. *A*, The protocol for immunotherapy is shown. *B*, A total of 5×10^5 TG-3-2B cells were first injected intradermally into HLA-A*2402/K^b mice (10 animals/group). When mean tumor diameter reached 5 mm, mice were given the treatment with the Hsp90 (50 μg)-survivin-2B$_{80-88}$ (50 μg) complex, survivin-2B$_{80-88}$ (50 μg) emulsified with IFA alone or PBS twice a week. *C*, The remaining 10 mice in each group were observed for survival.

of Hsp90-survivin-2B complexes represents the survivin-2B-specific antitumor effects in vivo. TG3-2B cells (2×10^5) were inoculated into the right hind limbs of HLA-A*2402/K^b transgenic mice and allowed to grow for 10 days (to around 5 mm in diameter). As shown in Fig. 4A, on days 9, 13, 16, and 20, mice were administered PBS, the survivin-2B$_{80-88}$ peptide (50 μg), or the

Hsp90 (50 μg)-survivin-2B$_{80-88}$ (50 μg) complex. As shown in Fig. 4B, vaccination with Hsp90-survivin-2B$_{80-88}$ significantly inhibited the growth of tumors in comparison to control vaccinations with survivin-2B$_{80-88}$ or PBS, (vs survivin-2B, $p = 0.034$, vs PBS, $p = 0.0007$). We also evaluated the effects of the Hsp90-survivin-2B peptide complex in providing a survival benefit. As shown in Fig. 4C, the results indicated that treatment with the Hsp90-survivin-2B peptide complex significantly increased the median survival time compared with the control mice (vs survivin-2B, $p = 0.016$, vs PBS, $p = 0.001$). Of note, 8 of 10 animals of the Hsp90-survivin-2B$_{80-88}$ complex-treated groups rejected the established tumors. Taken together, these results showed not only that the Hsp90-peptide complex induced strong CTL responses to the chaperoned peptide but also that these responses were sufficiently strong to generate therapeutic antitumor effects.

TAP-independent presentation of Hsp90-bound peptide in the context of MHC class I by BMDCs

To generalize the Hsp90-mediated cross-presentation, we used a well-characterized antigenic system, the VSV derived H-2K^b-restricted VSV8 dominant Ag. To test the peptide-binding capacity of purified human Hsp90, we used synthetic peptides VSV8 and a C-terminal extended version of VSV8, VSV-C (15 mer). First, we confirmed the in vitro generation of the Hsp90-VSV-C peptide complex (data not shown). Next, we tested whether in vitro-reconstituted Hsp90-VSV-C complexes were taken up and associated peptides were presented in the context of MHC class I molecules by immature BMDCs. The Hsp90-VSV-C peptide complex was
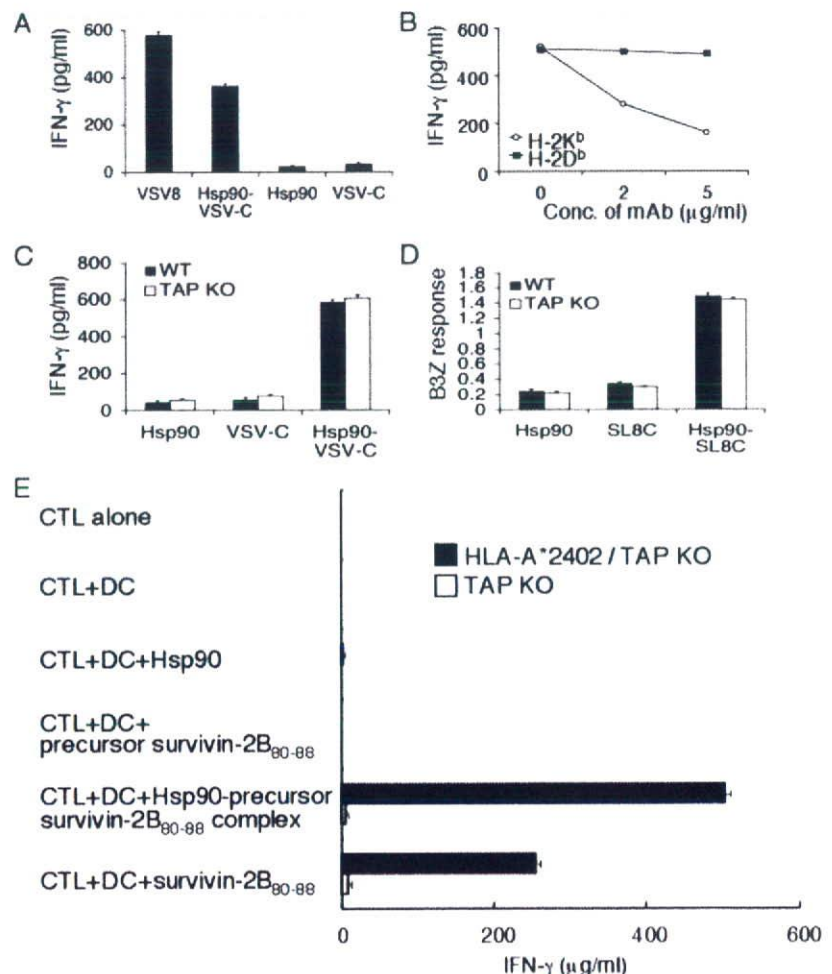

FIGURE 5. Precursor peptides chaperoned by Hsp90 are cross-presented via a TAP-independent pathway. *A*, VSV8, the Hsp90-VSV-C complex, Hsp90, or VSV-C was loaded to BMDCs for 2 h and a VSV8-specific CTL clone was added. IFN-γ in the culture supernatant was measured by ELISA. *B*, The anti-H-2K^b mAb, but not the H-2D^b mAb, inhibited cytotoxicity mediated by the VSV-8-specific CTL clone. *C*, BMDCs from the TAP$^{-/-}$ mouse could also process and present Hsp90-chaperoned VSV-C peptides efficiently as compared with BMDCs from the wild-type mouse. *D*, SL8 precursor peptide, SL8C was also processed and cross-presented by BMDCs via a TAP-independent pathway. *E*, HLA-A*2402-transduced TAP$^{-/-}$ BMDCs were able to cross-present Hsp90-chaperoned precursor survivin-2B$_{80-88}$ peptides in association with HLA-A*2402 molecules.
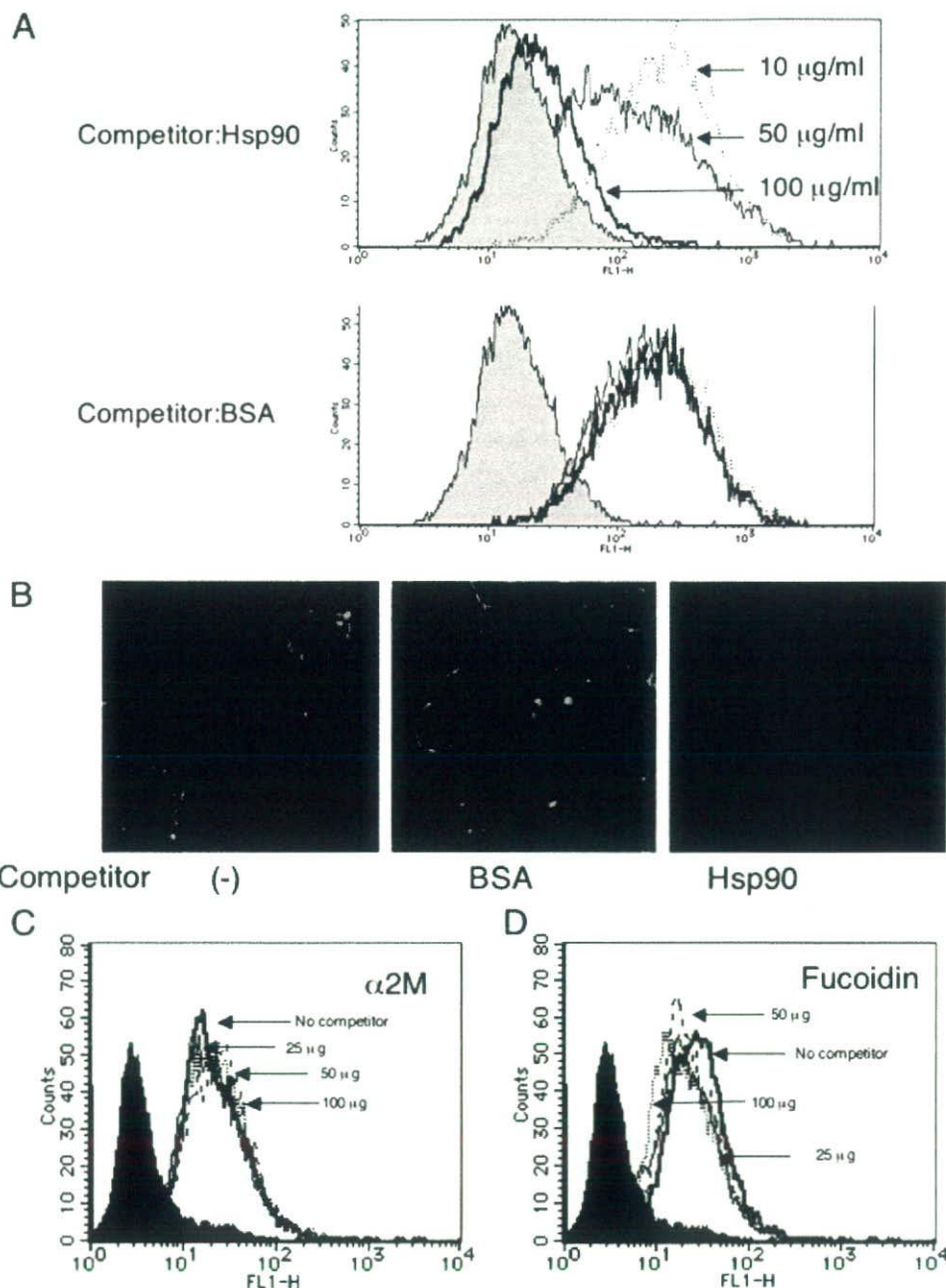
A

Competitor:Hsp90

Competitor:BSA

FIGURE 6. The Hsp90-peptide complex binds to immature BMDCs in a receptor-dependent fashion. *A*, BMDCs were incubated with the Alexa 488-labeled Hsp90-SL8C complex at 4°C to exclude endocytosis. Specific binding of the Hsp90-SL8C complex was observed and could be competed for by a 10-fold excess of unlabeled Hsp90. No inhibition was observed using an excess of up to 100-fold of BSA. *B*, BMDCs were incubated with unlabeled 50 μg/ml Hsp90 or 50 μg/ml BSA for 1 h on ice, then pulsed with 5 μg/ml Alexa 488-labeled Hsp90-SL8C complexes to DCs on ice for 1 h, washed with PBS, followed by acetone fixation and processing for confocal microscopy. *C* and *D*, The binding of the Hsp90-SL8C peptide complex to BMDCs was not inhibited by either the CD91 ligand α2M or the SR-A ligand fucoidin.

B

Competitor   (-)   BSA   Hsp90

C

D

cocultured with immature BMDCs for 2 h and fixed, followed by incubation with a VSV8-specific CTL clone. The culture supernatant was assayed for the production of IFN-γ. As shown in Fig. 5*A*, the Hsp90-VSV-C peptide complex was processed and presented by H-2K^b, and consequently recognized by the VSV8-specific CTL clone but not Hsp90 or VSV-C alone. In the presence of an anti-H-2K^b mAb but not an anti-H-2D^b mAb, during the presentation assay, the presentation of VSV8 to the specific CTL clone was clearly abolished (Fig. 5*B*). These data suggested that Hsp90 bound VSV-C peptide was processed to VSV8 within the cells with subsequent access to the MHC class I pathway.

Next, we investigated whether the Hsp90-mediated MHC class I pathway required functional TAP molecules. To test this, we used immature BMDCs derived from the TAP1$^{-/-}$ mouse. Surprisingly, BMDCs from the TAP1$^{-/-}$ mouse could also process and present the Hsp90-bound VSV-C peptide as efficiently as BMDCs from the wild-type mouse (Fig. 5*C*). Taking advantage of

the use of T cell hybridoma B3Z, we also tested another well-characterized H-2K^b-restricted OVA$_{257-264}$ Ag system. Hsp90 reconstituted in vitro with SL8C peptide (13mer, C-terminal extended version of SL8 (OVA$_{257-264}$)) was cocultured with BMDCs for 2 h, followed by incubation with an SL8-specific B3Z T cell hybridoma. As shown in Fig. 5*D*, the Hsp90-SL8C peptide complex but not Hsp90 or SL8C alone was processed and presented by H-2K^b, and recognized consequently by the B3Z T cell hybridoma in a TAP-independent manner.

Furthermore, we have confirmed that Hsp90-survivin-2B$_{75-93}$ precursor peptide complex was processed and presented by TAP$^{-/-}$ mice-derived BMDCs, which were retrovirally transduced with HLA-A*2402 cDNA, and consequently recognized by the survivin-2B$_{80-88}$-specific CTL clone but not Hsp90 or the survivin-2B$_{75-93}$ precursor peptide alone (Fig. 5*E*). These data demonstrated that a TAP-independent pathway was used for Hsp90-mediated MHC class I presentation.
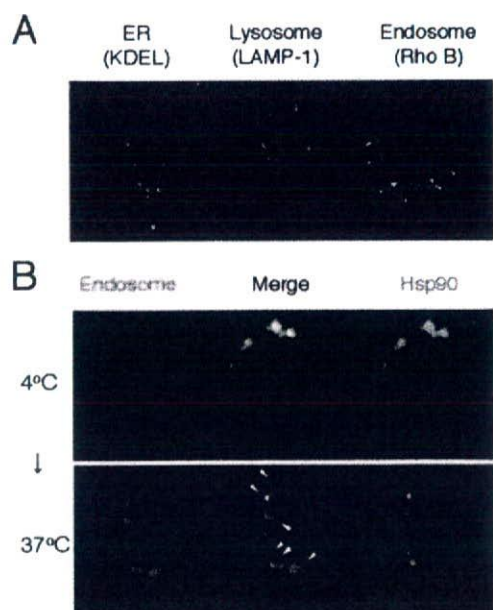
FIGURE 7. Intracellular localization of the Hsp90-SL8C peptide complex taken up by receptor-mediated endocytosis. *A*, Immature BMDCs were pulsed with Alexa 488-labeled Hsp90-SL8C complex for 2 h. After incubation, cells were fixed with cold acetone, stained with an anti-Rho B Ab (for early endosomes), anti-KDEL mAb (for ER), and anti-LAMP1 (for late endosomes and lysosomes) followed by Alexa 594-conjugated goat anti-rabbit IgG or anti-mouse IgG and visualized by laser confocal microscopy. *B*, Internalization of the Hsp90-peptide complex occurred via temperature-dependent endocytosis. BMDCs were treated either 4°C or at 37°C with 20 μg/ml Alexa 488-labeled Hsp90-SL8C complex for 10 min, washed with PBS, and fixed, then stained with the anti-Rho B Ab, followed by Alexa 594-conjugated goat anti-rabbit IgG and analyzed by laser confocal microscopy.

FIGURE 8. The Hsp90-peptide complex traffics to an endosome, where the precursor peptide might be processed, followed by the formation of a peptide-MHC class I complex. *A*, BMDCs were treated at either 4°C or at 37°C with the 20 μg/ml Alexa 488-labeled Hsp90-SL8C complex for 10 min, washed with PBS, and fixed, then stained using Alexa 594-conjugated anti-H-2K^b mAb. *B*, BMDCs were incubated with Hsp90-SL8C peptide complexes for 1 h, then fixed with ice-cold acetone for 1 min. DCs were incubated with mAb 2.4G2 to block FcR and then costained with Alexa 488-conjugated mAb 25D1.16 (for H-2K^b-SL8 complex) and Alexa 594-conjugated anti-Rho B Ab or anti-KDEL mAb.

Hsp90-peptide complex interacts with bone marrow-derived immature BMDCs in a receptor-dependent fashion

Recent experiments demonstrated that HSPs are able to interact specifically with macrophages, DC, and B cells. To test the specific binding of Hsp90-peptide complex to immature BMDCs, we incubated BMDCs with the Alexa 488-labeled Hsp90-SL8C complex at 4°C to exclude endocytosis. Using FACS analysis, we observed specific binding of Hsp90-peptide complexes to the cell surface that could be competed for by unlabeled Hsp90, but not by BSA (Fig. 6A). A 10-fold excess of unlabeled Hsp90 significantly inhibited the binding of Alexa 488-labeled Hsp90-SL8C complexes to BMDCs. No inhibition was observed using an excess of up to 100-fold of BSA. We then analyzed the competition experiments using the laser confocal microscopy. We have confirmed that after 1 h culture at 4°C, a temperature which blocks internalization, the Alexa 488-labeled Hsp90-SL8C complexes were found on the cell surface of immature BMDCs. Next, immature DCs were incubated with Alexa 488-labeled Hsp90-SL8C complexes, alone or in the presence of a 10-fold excess of unlabeled Hsp90 or BSA. As shown in Fig. 6B, competition with unlabeled Hsp90 significantly reduced the cell surface binding, whereas unlabeled BSA did not affect the binding as compared with the labeled Hsp90-peptide complex alone. These data demonstrated the presence of a specific receptor for Hsp90 that was expressed on immature BMDCs. Recently, CD91 (the α2M receptor), LOX-1, and scavenger receptor class-A (SR-A) were identified as the HSP receptors of APCs. Therefore, we have done the competition assay using α2M and fucoidin, which are known for the ligands of HSP receptors CD91 (for α2M), LOX-1, and SR-A (for fucoidin). The
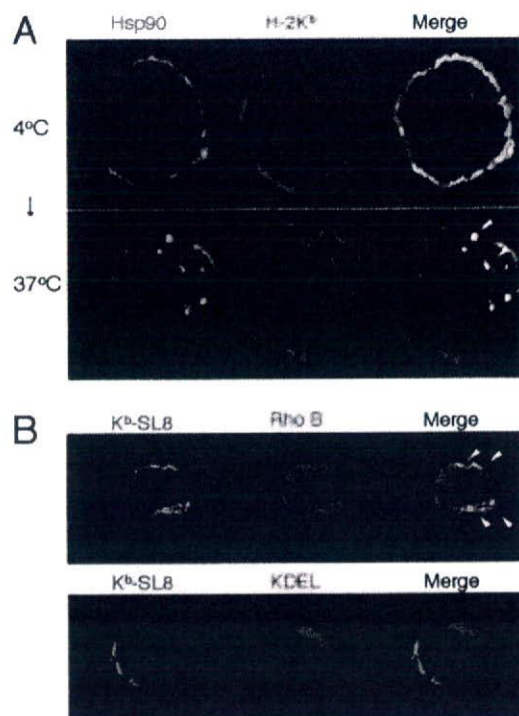
results showed that the twenty-fold concentration of either α2 macroglobulin (Fig. 6C) or fucoidin (Fig. 6D) was not able to compete the cell surface binding of Alexa Fluor 488-labeled Hsp90-SL8 complex. Therefore, we concluded that Hsp90 receptor was different from CD91 and scavenger receptors such as LOX-1 or SR-A in our experiments.

Endocytosed Hsp90-peptide complexes localize in the early endosome

Next, we were interested in addressing which compartments were involved in this processing and presentation of Hsp90-chaperoned precursor peptides within the BMDCs. We labeled human Hsp90-SL8C with Alexa Fluor 488. Labeled Hsp90-SL8C peptide complexes were then incubated with BMDCs for several time periods. After extensive washing to remove unbound proteins, cells were fixed with cold acetone and costained with an Ab against an organelle marker labeled with Alexa Fluor 594. Analysis by laser confocal microscopy of staining with the organelle marker revealed that the internalized Hsp90-SL8C complex localized in Rho B-positive early endosomes (Fig. 7A) but not late endosomes/lysosomes or endoplasmic reticulum (ER) after 10, 30, and 60 min of endocytosis (shown for 60 min in Fig. 7A). We traced Hsp90-SL8C complex after 90 and 120 min. It accumulated only in early endosomes and did not reach the stage of late endosomes/lysosomes (data not shown). In accordance with experiments using TAP 1$^{-/-}$ BMDCs, the lack of accumulation in the ER seemed to
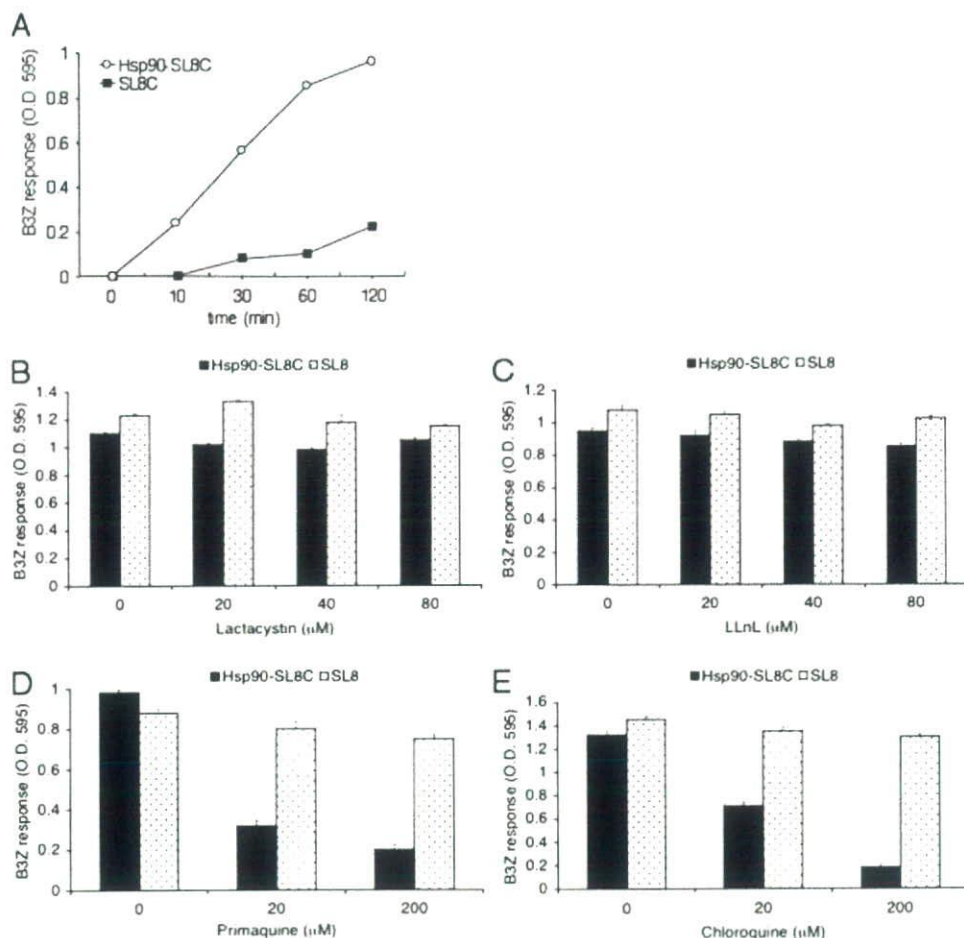
FIGURE 9. Membrane recycling and vacuolar acidification, but not proteasomal processing is required for cross-presentation of Hsp90-peptide complexes. *A*, Cross-presentation of Hsp90-chaperoned peptides by BMDC is very rapid response. *B–D*, BMDCs were preincubated with (*B*) lactacystin, (*C*) LLnL, (*D*) primaquine, or (*E*) chloroquine at 37°C for 2 h, then pulsed with Hsp90-SL8C complexes, SL8 peptide, or OVA protein for 2 h. The DCs were then fixed, washed, and cultured overnight with B3Z cells. The β-galactosidase activity was measured at the absorbance at 595 nm.

indicate that the Hsp90-mediated MHC class I pathway was independent of TAP. We also examined whether Hsp90-peptide complex accumulation in the early endosome was temperature-dependent endocytosis. As expected, at 4°C, labeled Hsp90-peptide complex remained on the cell surface (Fig. 7*B*), but internalization was evident after incubation at 37°C following a 10-min internalization period.

Extracellular Hsp90-peptide complexes and recycling MHC class I molecules are colocalized within early endosomes in BMDCs

To investigate in which compartment the Hsp90-chaperoned antigenic peptides bound to MHC class I molecules, we stained H-2K^b molecules and exogenous Hsp90-SL8C complexes. After 20 min of endocytosis, Alexa Fluor 488-labeled Hsp90-SL8C complexes colocalized with endocytosed H-2K^b molecules in the early endosome (Fig. 8*A*). This finding suggested that Hsp90-bound peptides might be transferred to MHC class I molecules in the early endosome where recycled MHC class I molecules from the plasma membrane are available. The peptide-MHC class I complexes generated in the early endosome would then be transported to the cell surface of the BMDCs, where specific CTLs recognize them.

Early endosomes are the compartment where Hsp90-bound precursor peptides are processed and transferred onto subcellular MHC class I molecules

To investigate in which compartment Hsp90-bound precursor peptides are processed and subsequently transferred onto MHC class I molecules, we used mAb 25D1.11 because this mAb recognizes

SL8 peptide-H-2K^b complexes (31). Hsp90-SL8C peptide complexes were pulsed onto BMDCs, subsequently fixed with acetone, and stained with mAb 25D1.11 labeled with Alexa Fluor 488 and anti-Rho B or anti-KEDL Abs coupled with Alexa Fluor 594. Consequently, we clearly observed that mAb 25D1.11 was detected only in the early endosomes and not in the ER (Fig. 8*B*). This fact indicated that Hsp90-bound precursor peptides were processed and transferred onto MHC class I within early endosomes, suggesting that recycling MHC class I molecules are required for efficient presentation of Hsp90-chaperoned peptides.

Kinetics of cross-presentation of Hsp90-chaperoned peptide by BMDCs

We evaluated the cross-presentation kinetics of the Hsp90-chaperoned precursor peptide by BMDCs. BMDCs were pulsed with the Hsp90-SL8C complex, sampled between 0 and 120 min and fixed with glutaraldehyde to terminate further Ag uptake and processing. After fixation, BMDCs were cocultured with B3Z T cell hybridoma. The presentation of Hsp90-chaperoned peptides was detected after a 10-min pulse (Fig. 9*A*), indicating that induction of immune responses can be achieved very rapidly. This is very important for Hsp90 as a danger signal. In contrast, presentation of free SL8C peptide was barely detectable within 2 h. In addition, to confirm that the Hsp90-mediated cross-presentation followed a TAP-independent pathway, we tested the effect of treating BMDCs with the proteasome inhibitor, lactacystin and LLnL. As expected, these agents did not affect the Hsp90-mediated cross-presentation by BMDCs (Fig. 9, *B* and *C*). Therefore, class I-presented peptides
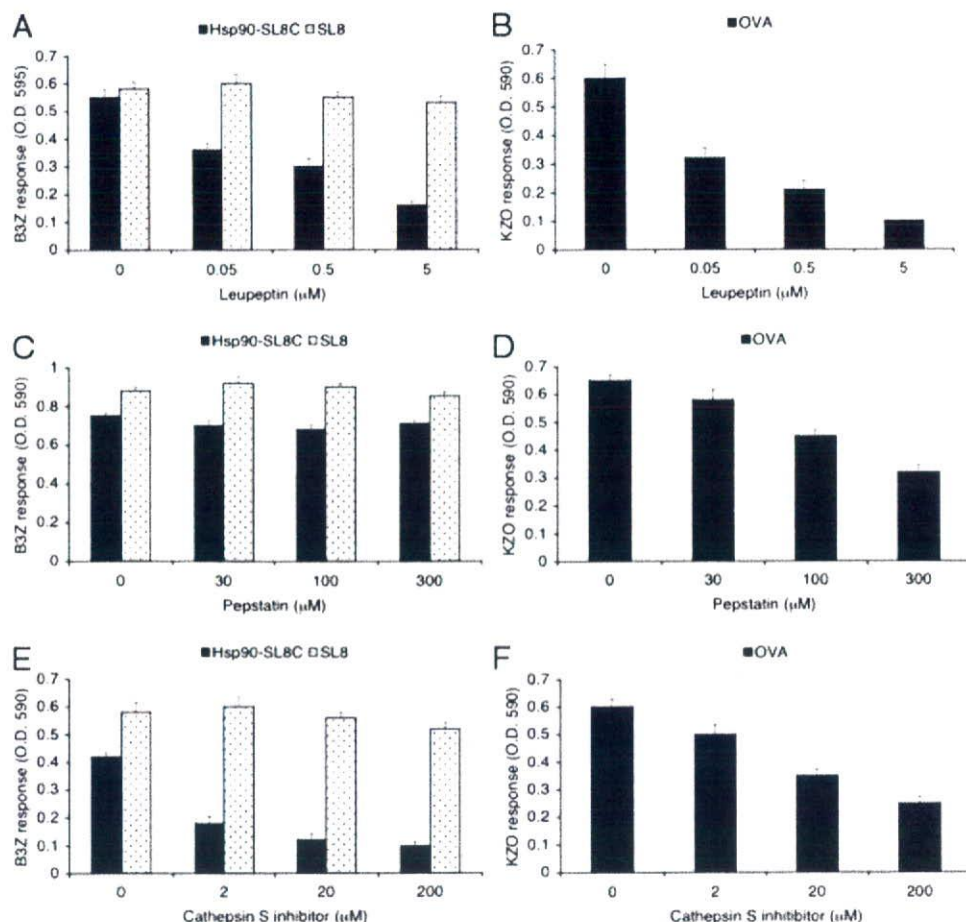
FIGURE 10. The Hsp90-chaperoned precursor peptide is processed by cysteine/serine proteases in the endosomes. *A–F*, DCs were preincubated with (*A* and *B*) leupeptin, (*C* and *D*) pepstatin, or (*E* and *F*) a cathepsin S inhibitor at 37°C for 2 h, then pulsed with Hsp90-SL8C complexes, SL8 peptide, or OVA protein for 2 h. The DCs were then fixed, washed, and cultured overnight with B3Z or KZO cells. The β-galactosidase activity was measured at the absorbance at 595 nm.

were generated from the Hsp90-precursor peptide complex through the endosomal pathway.

Hsp90-chaperoned peptides are transferred to recycling MHC class I molecules in early endosomes

Recycling of endocytosed MHC class I molecules back to the cell surface has been observed (32). Some of the recycling MHC class I molecules can be loaded into early endosomes with peptides derived from endocytosed molecules. Therefore, to confirm whether this presentation really used the recycling MHC class I molecules, we treated BMDCs with primaquine, which blocks the membrane recycling pathway. BMDCs incubated in the presence of this drug could not present the Hsp90-chaperoned SL8C (13 mer)-derived SL8 peptide (Fig. 9D). This result indicated that Hsp90-chaperoned precursor peptides or processed peptides could enter into recycling endosomes and be transferred onto recycling MHC class I molecules, which went back to the cell surface, resulting in the stimulation of B3Z T cell hybridoma. Furthermore, to analyze the involvement of vacuolar acidification of endosomal compartments, BMDCs were incubated with Hsp90-SL8C precursor peptide complexes in the presence of chloroquine, a known inhibitor of acidification of endosomal compartments. Chloroquine treatment resulted in strong inhibition of the Hsp90-mediated presentation, without affecting SL8 peptide presentation, showing that acidification of endosomal compartments was necessary for Hsp90-chaperoned precursor peptide processing (Fig. 9E).

Hsp90-chaperoned peptides are processed by endosomal protease

We used protease inhibitors to investigate how proteolytic processes were involved in this Hsp90-mediated TAP-independent

cross-presentation pathway. We found that, in wild-type BMDC, a broadly active cysteine protease inhibitor, leupeptin, almost completely inhibited the cross-presentation of Hsp90-SL8C precursor peptide complexes (Fig. 10A). In contrast, the aspartic protease inhibitor pepstatin did not affect the cross-presentation (Fig. 10C). The concentration of leupeptin or pepstatin used was sufficient to inhibit cysteine proteases or aspartic protease because it completely blocked the presentation of soluble OVA on MHC class II molecules detected by I-A^k-specific CD4$^+$ T cell hybridoma KZO (Fig. 10, *B* and *D*). These results indicated that cysteine proteases are required for the Hsp90-mediated cross-presentation.

We next studied the role of cathepsins in the Hsp90-mediated vacuolar cross-presentation. Cathepsins S, B, and L are known to be the major cysteine proteases in endocytic compartments. We therefore examined the roles of various cathepsins in this pathway. A cathepsin B- or cathepsin L-specific inhibitor did not affect Hsp90-mediated cross-presentation (data not shown), whereas a cathepsin S inhibitor clearly blocked cross-presentation (Fig. 10E), as well as the presentation of soluble OVA on MHC class II molecules detected by KZO T cell hybridoma (Fig. 10F). Cathepsin S is preferentially expressed in APCs, including DCs, macrophages, and B cells within endocytic compartments. Therefore, our data indicated that cathepsin S was a critical enzyme in TAP-independent Hsp90-mediated cross-presentation to MHC class I molecules and that antigenic precursor peptides were indeed processed to epitope peptides, followed by association with MHC class I molecules in endosomal compartments.

Hsp90-protein Ag complex is cross-presented by BMDCs

Lastly, we evaluated cross-presentation of the in vitro-generated Hsp90-OVA protein complex. In vitro generation of Hsp90-OVA
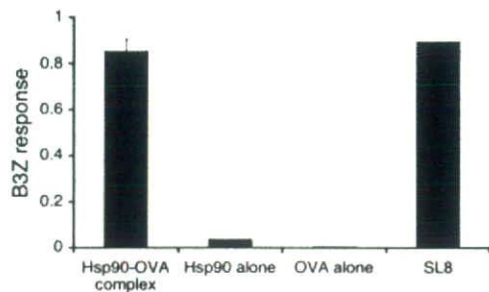
FIGURE 11. The Hsp90-OVA complex is presented by BMDCs through the MHC class I pathway. BMDCs were pulsed with Hsp90 alone, OVA alone, a complex of them or SL8 for 2 h at 37°C, then fixed, washed, and cultured overnight with B3Z. The β-galactosidase activity was measured at the absorbance at 595 nm.

complexes was performed and confirmed according to the method described in *Materials and Methods*. BMDCs were pulsed with Hsp90 alone, free OVA, or a complex of them generated in vitro for 2 h at 37°C, then fixed, washed, and cultured with B3Z CD8$^+$ T cell hybridoma. Hsp90-OVA elicited strong B3Z responses, while Hsp90 or OVA alone did not induce a B3Z response (Fig. 11). Thus, Hsp90-chaperoned protein Ag as well as peptide is efficiently cross-presented by BMDCs.

Discussion

We have shown here that Hsp90-peptide complexes could induce strong CTL responses, leading to efficient antitumor immunity via cross-presentation pathway. Interestingly, Hsp90-mediated cross-presentation is independent of TAP and sensitive to chloroquine, suggesting that processing and loading of peptides onto MHC class I occurs via the endosomal pathway. Although Binder et al. (33) have demonstrated that exogenous Hsp70 and gp96-mediated cross-priming is dependent on the TAP system in the peritoneal macrophage and macrophage cell line RAW264.7, we used immature BMDCs for Ag-presentation assay. In addition, they used N-[1-(2,3-dioleoyloxy)propyl]-N,N,N-trimethylammonium methylsulfate (DOTAP) for introduction of HSP-peptide complexes into the cytosol of the macrophages. By contrast, we used exogenous Hsp90-peptide complex-pulsed BMDCs for the detection of the in vitro cross-presentation so as to mimic the situation that HSP-peptide complexes would be released into the extracellular milieu as a consequence of pathological cell death. In fact, Schoenberger et al. (34) demonstrated that cells deficient in TAP were still able to cross-present as efficiently as wild-type cell.

We have shown that exogenously loaded Hsp90 trafficked to early endosomes via receptor-mediated endocytosis and colocalized with recycling MHC class I molecules in the early endosomes where the exchange of the Hsp90-chaperoned-peptides might occur. Recent reports have identified several pathways wherein peptides exchange onto recycling MHC class I molecules occurs within early endosomal compartments (32, 35). Such trafficking pathways for recycling MHC class I molecules bear broad similarities to that observed for Hsp90. Therefore, we propose that, for the Hsp90-chaperoned peptide, the early endosome is a site for peptide exchange onto class I molecules for subsequent presentation. In addition, we have shown that the cysteine protease cathepsin S plays an important role in the generation of MHC class I peptides in endosomes. Rock and colleagues (36) have demonstrated that cathepsin S is a key enzyme for the generation of exogenous OVA-derived SL8 peptide, which is presented by a TAP-independent pathway. These facts indicate that endosomal cathepsin S might be necessary for the generation of Ag peptides,

cross-presented by DCs. Further research defining the precise mechanisms of peptide exchange and processing may reveal a new paradigm for cross-presentation. Nicchitta and colleagues (5) have shown that gp96 internalizes by receptor-mediated endocytosis trafficked to an FcR and MHC class I-positive endocytic compartment and does not access the ER of BMDCs. These observations are consistent with our data. Taken together, it is suggested that BMDCs bear cell-surface receptors that are capable of directing HSP-peptide complexes into the class I Ag-presentation pathway. We are currently investigating the Hsp90-specific receptor on the APCs, which is responsible for the cross-presentation.

In contrast, immunization with the Hsp70-peptide complex elicited only weak CTL responses even though an Hsp70-antigenic peptide complex could be generated. The mechanistic details causing drastic differences between Hsp90 and Hsp70 in CTL induction remain to be determined.

These results indicate that Hsp90 serves as a powerful danger signal and elicits prompt protective immune responses against infection and cellular stress. Although, compared with the TAP-dependent pathway, the TAP-independent pathway is less effective under stress conditions, very rapid generation of protective immune responses could be beneficial against life-threatening events.

We have also demonstrated that Hsp90-chaperoned Ags cross-presented by BMDCs elicit strong Ag-specific CTL induction in vivo and an antitumor therapeutic effect. Although we used human tumor Ag survivin-2B as a surrogate Ag in the HLA-A*2402 transgenic mouse system, leading our tumor model highly immunogenic, treatment with Hsp90-survivin-2B$_{80-88}$ complexes showed significant therapeutic effect compared with treatment with survivin-2B$_{80-88}$ emulsified in IFA. The results suggested that Hsp90 might be a promising candidate for a well-tolerated adjuvant. Taken together, these results suggest new avenues for Hsp90-based immunotherapy in viral infection as well as anticancer vaccination.

Disclosures

The authors have no financial conflict of interest.

References

1. Srivastava, P. 2002. Interaction of heat shock proteins with peptides and antigen presenting cells: chaperoning of the innate and adaptive immune responses. *Annu. Rev. Immunol.* 20: 395–425.
2. Castellino, F., P. E. Boucher, K. Eichelberg, M. Mayhew, J. E. Rothman, A. N. Houghton, and R. N. Germain. 2000. Receptor-mediated uptake of antigen/heat shock protein complexes results in major histocompatibility complex class I antigen presentation via two distinct processing pathways. *J. Exp. Med.* 191: 1957–1964.
3. Singh-Jasuja, H., R. E. Toes, P. Spee, C. Munz, N. Hilf, S. P. Schoenberger, P. Ricciardi-Castagnoli, J. Neefjes, H. G. Rammensee, D. Arnold-Schild, and H. Schild. 2000. Cross-presentation of glycoprotein 96-associated antigens on major histocompatibility complex class I molecules requires receptor-mediated endocytosis. *J. Exp. Med.* 191: 1965–1974.
4. Berwin, B., and C. V. Nicchitta. 2001. To find the road traveled to tumor immunity: the trafficking itineraries of molecular chaperones in antigen-presenting cells. *Traffic* 2: 690–697.
5. Berwin, B., M. F. Rosser, K. G. Brinker, and C. V. Nicchitta. 2002. Transfer of GRP94 (Gp96)-associated peptides onto endosomal MHC class I molecules. *Traffic* 3: 358–366.
6. Binder, R., D. Han, and P. Srivastava. 2000. CD91: a receptor for heat shock protein gp96. *Nat. Immunol.* 1: 151–155.
7. Becker, T., F. U. Hartl, and F. Wieland. 2002. CD40, an extracellular receptor for binding and uptake of Hsp70-peptide complexes. *J. Cell. Biol.* 158: 1277–1285.
8. Vabulas, R. M., P. Ahmad-Nejad, S. Ghose, C. J. Kirschning, R. D. Issels, and H. Wagner. 2002. HSP70 as endogenous stimulus of the Toll/interleukin-1 receptor signal pathway. *J. Biol. Chem.* 277: 15107–15112.
9. Delneste, Y., G. Magistrelli, J. Gauchat, J. Haeuw, J. Aubry, K. Nakamura, N. Kawakami-Honda, L. Goetsch, T. Sawamura, J. Bonnefoy, and P. Jeannin.

2002. Involvement of LOX-1 in dendritic cell-mediated antigen cross-presentation. *Immunity* 17: 353–362.

10. Berwin, B., J. P. Hart, S. Rice, C. Gass, S. V. Pizzo, S. R. Post, and C. V. Nicchitta. 2003. Scavenger receptor-A mediates gp96/GRP94 and calreticulin internalization by antigen-presenting cells. *EMBO J.* 22: 6127–6136.

11. Basu, S., R. J. Binder, T. Ramalingam, and P. K. Srivastava. 2001. CD91 is a common receptor for heat shock proteins gp96, hsp90, hsp70, and calreticulin. *Immunity* 14: 303–313.

12. Tamura, Y., P. Peng, K. Liu, M. Daou, and P. K. Srivastava. 1997. Immunotherapy of tumors with autologous tumor-derived heat shock protein preparations. *Science* 278: 117–120.

13. Blachere, N. E., Z. Li, R. Y. Chandawarkar, R. Suto, N. S. Jaikaria, S. Basu, H. Udono, and P. K. Srivastava. 1997. Heat shock protein-peptide complexes, reconstituted in vitro, elicit peptide-specific cytotoxic T lymphocyte response and tumor immunity. *J. Exp. Med.* 186: 1315–1322.

14. Sato, K., Y. Torimoto, Y. Tamura, M. Shindo, H. Shinzaki, K. Hirai, and Y. Kohgo. 2001. Immunotherapy using heat-shock protein preparations of leukemia cells after syngeneic bone marrow transplantation in mice. *Blood* 98: 1852–1857.

15. Moroi, Y., M. Mayhew, J. Trcka, M. H. Hoe, Y. Takechi, F. U. Hartl, J. E. Rothman, and A. N. Houghton. 2000. Induction of cellular immunity by immunization with novel hybrid peptides complexed to heat shock protein 70. *Proc. Natl. Acad. Sci. USA* 97: 3485–3490.

16. Castelli, C., A. M. Ciupitu, F. Rini, L. Rivoltini, A. Mazzocchi, R. Kiessling, and G. Parmiani. 2001. Human heat shock protein 70 peptide complexes specifically activate antimelanoma T cells. *Cancer Res.* 61: 222–227.

17. Noessner, E., R. Gastpar, V. Milani, A. Brandl, P. J. Hutzler, M. C. Kuppner, M. Roos, E. Kremmer, A. Asea, S. K. Calderwood, and R. D. Issels. 2002. Tumor-derived heat shock protein 70 peptide complexes are cross-presented by human dendritic cells. *J. Immunol.* 169: 5424–5432.

18. Milani, V., E. Noessner, S. Ghose, M. Kuppner, B. Ahrens, A. Scharner, R. Gastpar, and R. D. Issels. 2002. Heat shock protein 70: role in antigen presentation and immune stimulation. *Int. J. Hyperthermia* 18: 563–575.

19. Ueda, G., Y. Tamura, I. Hirai, K. Kamiguchi, S. Ichimiya, T. Torigoe, H. Hiratsuka, H. Sunakawa, and N. Sato. 2004. Tumor-derived heat shock protein 70-pulsed dendritic cells elicit tumor-specific cytotoxic T lymphocytes (CTLs) and tumor immunity. *Cancer Sci.* 95: 248–253.

20. Basu, S., R. J. Binder, R. Suto, K. M. Anderson, and P. K. Srivastava. 2000. Necrotic but not apoptotic cell death releases heat shock proteins, which deliver a partial maturation signal to dendritic cells and activate the NF-κB pathway. *Int. Immunol.* 12: 1539–1546.

21. Somersan, S., M. Larsson, J. F. Fonteneau, S. Basu, P. Srivastava, and N. Bhardwaj. 2001. Primary tumor tissue lysates are enriched in heat shock proteins and induce the maturation of human dendritic cells. *J. Immunol.* 167: 4844–4852.

22. Bethke, K., F. Staib, M. Distler, U. Schmitt, H. Jonuleit, A. H. Enk, P. R. Galle, and M. Heike. 2002. Different efficiency of heat shock proteins (HSP) to activate human monocytes and dendritic cells: superiority of HSP60. *J. Immunol.* 169: 6141–6148.

23. Gallucci, S., and P. Matzinger. 2001. Danger signals: SOS to the immune system. *Curr. Opin. Immunol.* 13: 114–119.

24. Udono, H., and P. K. Srivastava. 1994. Comparison of tumor-specific immunogenicities of stress-induced proteins gp96, hsp90, and hsp70. *J. Immunol.* 152: 5398–5403.

25. Kunisawa, J., and N. Shastri. 2006. Hsp90α chaperones large C-terminally extended proteolytic intermediates in the MHC class I antigen processing pathway. *Immunity* 24: 523–534.

26. Kitamura, T., Y. Koshino, F. Shibata, T. Oki, H. Nakajima, T. Nosaka, and H. Kumagai. 2003. Retrovirus-mediated gene transfer and expression cloning: powerful tools in functional genomics. *Exp. Hematol.* 31: 1007–1014.

27. Morita, S., T. Kojima, and T. Kitamura. 2000. Plat-E: an efficient and stable system for transient packaging of retroviruses. *Gene Ther.* 7: 1063–1066.

28. Hirohashi, Y., T. Torigoe, A. Maeda, Y. Nabeta, K. Kamiguchi, T. Sato, J. Yoda, H. Ikeda, K. Hirata, N. Yamanaka, and N. Sato. 2002. An HLA-A24-restricted cytotoxic T lymphocyte epitope of a tumor-associated protein, survivin. *Clin. Cancer Res.* 8: 1731–1739.

29. Idenoue, S., Y. Hirohashi, T. Torigoe, Y. Sato, Y. Tamura, H. Hariu, M. Yamamoto, T. Kurotaki, T. Tsuruma, H. Asanuma, et al. 2005. A potent immunogenic general cancer vaccine that targets survivin, an inhibitor of apoptosis proteins. *Clin. Cancer Res.* 11: 1474–1482.

30. Gotoh, M., H. Takasu, K. Harada, and T. Yamaoka. 2002. Development of HLA-A2402/Kᵇ transgenic mice. *Int. J. Cancer* 100: 565–570.

31. Porgador, A., J. W. Yewdell, Y. Deng, J. R. Bennink, and R. N. Germain. 1997. Localization, quantitation, and in situ detection of specific peptide-MHC class I complexes using a monoclonal antibody. *Immunity* 6: 715–726.

32. Gromme, M., F. G. Uytdehaag, H. Janssen, J. Calafat, R. S. van Binnendijk, M. J. Kenter, A. Tulp, D. Verwoerd, and J. Neefjes. 1999. Recycling MHC class I molecules and endosomal peptide loading. *Proc. Natl. Acad. Sci. USA* 96: 10326–10331.

33. Binder, R. J., N. E. Blachere, and P. K. Srivastava. 2001. Heat shock protein-chaperoned peptides but not free peptides introduced into the cytosol are presented efficiently by major histocompatibility complex I molecules. *J. Biol. Chem.* 276: 17163–17171.

34. Schoenberger, S. P., E. I. van der Voort, G. M. Krietemeijer, R. Offringa, C. J. Melief, and R. E. Toes. 1998. Cross-priming of CTL responses in vivo does not require antigenic peptides in the endoplasmic reticulum of immunizing cells. *J. Immunol.* 161: 3808–3812.

35. Kleijmeer, M. J., J. M. Escola, F. G. UytdeHaag, E. Jakobson, J. M. Griffith, A. D. Osterhaus, W. Stoorvogel, C. J. Melief, C. Rabouille, and H. J. Geuze. 2001. Antigen loading of MHC class I molecules in the endocytic tract. *Traffic* 2: 124–137.

36. Shen, L., L. J. Sigal, M. Boes, and K. L. Rock. 2004. Important role of cathepsin S in generating peptides for TAP-independent MHC class I cross presentation in vivo. *Immunity* 21: 155–165.

Interferon γ assay for detecting latent tuberculosis infection in rheumatoid arthritis patients during infliximab administration

Hiroki Takahashi · Katsunori Shigehara · Motohisa Yamamoto · Chisako Suzuki ·
Yasuyoshi Naishiro · Yasunori Tamura · Yoshihiko Hirohashi · Noriyuki Satoh ·
Noriharu Shijubo · Yasuhisa Shinomura · Kohzoh Imai

Abstract In rheumatoid arthritis (RA) patients treated with infliximab (IFX), QuantiFERON-TB Gold (QFT-G), an interferon γ assay for diagnosing tuberculosis infection, was performed to compare its effectiveness to conventional diagnostic procedures (tuberculin skin test, imaging and medical history) in diagnosing latent tuberculosis infection (LTBI). QFT-G was measured bimonthly in 14 rheumatoid arthritis patients during IFX treatment. Seven of 14 patients were confirmed as LTBI positive by at least one method. Of these, four were positive on QFT-G during the study period, and two were positive before the start of IFX administration. For two of the four QFT-G-positive patients, LTBI was diagnosed only by QFT-G. The rate of agreement between QFT-G and conventional procedures was 64.3%. A total of 5% of QFT-G tests were impossible to judge due to decreased reactions in the positive control. These results suggest that QFT-G is able to detect LTBI in RA patients overlooked by conventional methods. Conventional procedures and QFT-G should be employed in parallel, and LTBI should be assumed when one technique gives a positive result.

Keywords Interferon γ assay · Latent tuberculosis infection · Rheumatoid arthritis · Infliximab · Tuberculin skin test

H. Takahashi (✉) · M. Yamamoto · C. Suzuki ·
Y. Naishiro · Y. Shinomura
First Department of Internal Medicine,
Sapporo Medical University School of Medicine,
South 1, West 16, Chuo-ku, Sapporo 060-8543, Japan
e-mail: htakahas@sapmed.ac.jp

K. Shigehara · Y. Tamura · Y. Hirohashi · N. Satoh
First Department of Pathology, Sapporo Medical University
School of Medicine, Sapporo, Japan

K. Shigehara
Health Management Division, Sapporo Hospital,
Hokkaido Railway Co, Sapporo, Japan

Y. Naishiro
Department of Biomedical Engineering,
Sapporo Medical University School of Medicine, Sapporo, Japan

N. Shijubo
Department of Respiratory Medicine, Sapporo Hospital,
Hokkaido Railway Co, Sapporo, Japan

K. Imai
Sapporo Medical University, Sapporo, Japan

Introduction

As a therapeutic drug for rheumatoid arthritis (RA), anti-TNF inhibitors show prompt, specific anti-inflammatory action and joint destruction depression effects, and have thus become important in intractable RA treatment [1]. On the other hand, the frequent occurrence of opportunistic infections is of concern due to the artificial inhibition of TNF. As anti-TNF inhibitors have become more widely used in RA treatment, increases in the incidence of tuberculosis infection have been reported [2, 3]. Because these cases represent reactivation of endogenous infection, onset may be prevented by prophylactic administration of isoniazid (INH) if latent tuberculosis infection (LTBI) can be adequately detected before initiating anti-TNF therapy [4]. However, conventional techniques are insufficient to identify LTBI, i.e., in-depth history (history of treatment, contact with active TB patients), imaging (chest X-ray and CT) and tuberculin skin test (TST). Furthermore, it is difficult to

diagnose LTBI based on the results of TST alone, as the Bacillus Calmette-Guerin (BCG) vaccine is widely used in various countries, including Japan [5].

Therefore, an interferon γ assay for ESAT-6 and CFP-10, both of which are specific proteins for *Mycobacterium tuberculosis* and are not present in BCG, has been put to practical use in recent years. The advantages of interferon γ assay in the diagnosis of LTBI are reported to be high in specificity and sensitivity [6–8]. However, there have been no reports regarding the utility of interferon γ assay in anti-TNF inhibitor treatment for RA. We performed an observational study focusing on the utility of LTBI monitoring by QuantiFERONTM-TB Gold test (QFT-G, Cellestis, Australia), an interferon γ assay, in RA patients scheduled for treatment or undergoing treatment with infliximab (IFX), an anti-TNF inhibitors, and the results were compared with conventional diagnostic approaches. In addition, we examined the serial changes in measurement of QFT-G during IFX administration.

Materials and methods

Study population

We performed an observational study of 14 patients with RA in whom the presence of active tuberculosis infection was excluded prior to initiation of IFX administration at Sapporo Medical University Hospital. For this, QFT-G measurement was started before IFX administration in three patients. QFT-G measurement was started before the fifth administration of IFX in two patients and before the seventh administration of IFX in nine patients. Chronologic measurement of QFT was performed in alternate months. The study was approved as a clinical audit by the hospital research committee and all participants provided written informed consent. We estimated patients as being LTBI according to the following conditions and INH prophylaxis was performed [9]; history of tuberculosis treatment or close contact with an infected person, abnormal findings on chest X-ray suggestive of old tuberculosis (calcification shadows more than 5 mm, pleural thickening, linear opacities), TST with redness at least 20 mm in diameter or the presence of induration, or positive result on QFT-G (more than 0.35 IU/ml). Treatment with INH was initiated at 300 mg/day and continued with pyridoxine supplementation.

Patient characteristics (Table 1)

The mean age was 48.6 years (range 18–64 years), and the male/female ratio was 3:11. Methotrexate (MTX) was used in all patients and prednisolone was administered at an average of 5.8 mg/day in 12 of 14 patients. There was no

Table 1 Patient characteristics

Case	Age (Year/Sex)	NO of IFX treatment	Medications except MTX	Prophylaxis by INH
1	63/Male	10	PSL	+
2	50/Male	1	PSL	+
3	50/Female	8	PSL	±
4	46/Female	12	PSL	−
5	44/Female	12	PSL	−
6	64/Female	18	PSL	+
7	61/Female	17	−	+
8	51/Female	24	CsA	−
9	18/Female	18	PSL	−
10	50/Female	18	PSL	−
11	35/Female	18	PSL	−
12	51/Female	18	PSL	−
13	43/Female	18	PSL	−
14	54/Male	18	PSL	−

IFX Infliximab, *MTX* methotrexate, *PSL* prednisolone, *CsA* cyclosporine A, *INH* isoniazid

change about medications just before start of IFX therapy. The average number of treatments with IFX was 15 (range 1–24). IFX treatment was canceled in case 2 due to a history of tuberculous lymphadenitis and positive QFT-G after initiation of IFX treatment. INH prophylaxis was performed in cases 1, 2, 3, 6 and 7 by the condition mentioned above. Of these, INH administration was started based on medical history in case 3, but liver dysfunction developed, and INH was terminated in four weeks. However, INH was not used in spite of positive result of TST in case 8 because IFX treatment had been initiated before the release of Japanese guidelines for prescribing anti-TNF agents. INH was not used in case 4 due to the transient positivity of QFT-G.

QuantiFERON-TB gold

Testing was performed at the First Department of Pathology according to the manufacturer's recommendations. Briefly, the test consisted of a negative control (nil well, i.e., whole blood without antigens or mitogen), a positive control (mitogen well, i.e., whole blood stimulated with the mitogen phytohemagglutinin [PHA]) and two sample wells, i.e., whole blood stimulated with either of the *M. tuberculosis*-specific antigens, Early Secretory Antigen Target 6 (ESAT-6) or Culture Filtrate Protein 10 (CFP-10). Whole blood specimens were incubated for 16–20 h (overnight) at 37°C in a humidified atmosphere. IFN γ levels in the nil well were considered background and were subtracted from the results of the mitogen well and the antigen-stimulated wells. The results were considered positive if the concentration

of IFN γ in the sample well after stimulation with ESAT-6 and/or CFP-10 was greater than or equal to 0.35 IU/ml (after subtracting the value of the nil well), regardless of the results of the positive control (mitogen well). The results were considered negative if the response to the specific antigens (after subtracting the value of the nil well) was less than 0.35 IU/ml and if the IFN γ levels of the positive control (after subtracting the value of the nil well) were greater than or equal to 0.5 IU/ml. The results were considered indeterminate if both antigen-stimulated sample wells were negative (i.e., <0.35 IU/ml after subtracting the value of the nil well) and if the value of the positive control well was less than 0.5 IU/ml after subtracting the value of the nil well.

Results

QFT-G measurement results (Table 2)

Tuberculosis infection including extrapulmonary involvement was not seen during the study period. The mean observation period after initiation of IFX treatment was 28.3 months (range 13–44 months). The average number of QFT-G measurements was 4.3 (range 2–8). In cases 1–3, measurement of QFT-G was performed of before the start of IFX administration. Positive QFT-G was observed in four patients (cases 1, 2, 4 and 7) irrespective of IFX administration, and two patients were positive on QFT-G before IFX administration. Indeterminate results were observed in three of 60 tests (5%) due to inadequate production of IFN γ by PHA stimulation. Of these, case 8 recorded indeterminate results twice, and this patient was treated with cyclosporine A together with MTX.

QFT-G in LTBI detection and comparison with conventional diagnostic procedures (Table 3)

When it was defined as LTBI by positive result of either QFT-G or conventional diagnostic procedures, seven patients were taken as LTBI. QFT-G was positive in four of 14 patients. As for two of four patients, existence of LTBI was proved only by QFT-G. The number of cases diagnosed as having LTBI by TST, imaging (chest X-ray, CT), and medical history was 4/14, 1/14 and 4/14, respectively. Medical histories supporting diagnosis of LTBI included treatment history of pulmonary tuberculosis (two cases), tuberculous lymphadenitis (one case) and family history with childhood tuberculosis in patient's son (one case). In QFT-G and traditional approaches (TST, chest X-ray, medical history), both were negative in seven cases and both were positive in two cases. Accordingly, the rate of agreement was 64.3%.

Table 2 QFT-G measurement results

Case	NO of QFT assay	QFT-G assay			Observational period (M)
		Negative	Positive	Indeterminate	
1	7	0	7	0	16
2	2	0	1	0	31
3	4	3	0	0	13
4	4	2	1	1	20
5	2	2	0	0	20
6	7	7	0	0	32
7	8	2	4	0	29
8	4	2	0	2	44
9	5	4	0	0	32
10	2	2	0	0	32
11	4	3	0	0	31
12	3	3	0	0	32
13	4	3	0	0	32
14	4	3	0	0	32

QFT-G QuantiFERON-TB, *INH* isoniazid

Table 3 Comparison of QFT-G with other procedures for LTBI diagnosis

Case	QFT results		TST test	Chest X-ray	Medical history
	Pretreatment	During treatment			
1	+	+	−	−	−
2	+	−	+	−	+
3	−	−	+	−	+
4	ND	+	−	−	−
5	ND	−	−	−	−
6	ND	−	−	+	+
7	ND	+	+	−	+
8	ND	−	+	−	−
9	ND	−	−	−	−
10	ND	−	−	−	−
11	ND	−	−	−	−
12	ND	−	−	−	−
13	ND	−	−	−	−
14	ND	−	−	−	−

LTBI Latent tuberculosis infection, *QFT-G* quantiFERON-TB, *TST* tuberculin skin test, *ND* not determine

Chronologic changes in QFT-G during administration of anti-TNF inhibitor (Fig. 1)

Measurement of QFT-G was repeated more than four times in nine patients. The chronologic changes are shown in Fig. 1 according to each antigen (ESAT-6 and CFP-10). INH prophylaxis was performed in cases 1, 2, 3, 6 and 7.
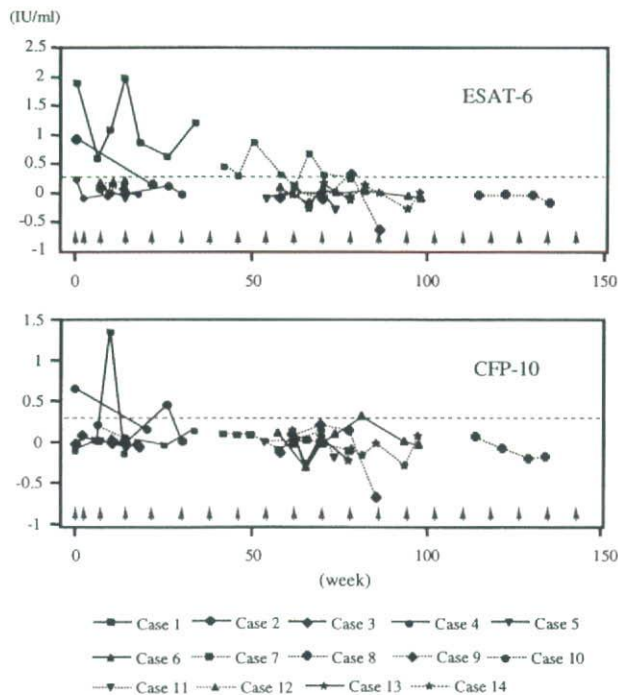
(IU/ml)

Fig. 1 Serial measurement of QFT-G during treatment with infliximab. QFT-G values in the nine cases that were measured more than four times are shown according to each antigen. *QFT-G Quanti-FERON-TB Gold, *ESAT-6* early secretory antigen target 6, *CFP-10* culture filtrate protein 10

QFT-G levels (ESAT-6 in particular) tended to decrease after initiating INH in case 2 and case 7. On the other hand decreased levels on QFT-G were not observed in case 1, in which QFT-G was positive before administration of IFX. Drastic changes were absent during the observational period in cases giving negative results at the beginning of IFX administration.

Discussion

Due to the drawbacks of LTBI diagnosis by conventional approaches (medical history, imaging and TST), QFT-G, an interferon γ assay for *M. tuberculosis*-specific ESAT-6 and CFP-10, was developed. QFT-G is reported to have high specificity and sensitivity for diagnosis of tuberculosis infection, as it is not affected by BCG vaccination [8]. According to recent reports, interferon γ assay exceeded TST in both sensitivity and specificity in the diagnosis of tuberculosis infection in immunocompetent individuals [6, 7]. To our knowledge, however, there have been no reports regarding the utility of interferon γ assay in LTBI detection with anti-TNF inhibitor use, and even the CDC guidelines do not mention the utility of QFT-G [10, 11]. In order to compare QFT-G with conventional approaches for

the diagnosis of LTBI during IFX administration, we thus performed this observational study.

Although it was impossible to calculate the sensitivity and specificity due to the lack of a gold standard for LTBI, the present study showed that seven patients were judged as having LTBI according to conditions described above. Accordingly, the rate of agreement between conventional methods and QFT-G was 64.3%. On the other hand, excellent agreement between TST and QFT-G was reported (more than 90%) in contacts in a tuberculosis outbreak [8, 12, 13]. This difference may be explained by the following problems related to TST; false positivity due to BCG vaccination and atypical mycobacterial infection, and false negativity caused by immunosuppression (aging, immuno-suppressive drugs such as corticosteroid, diabetes mellitus and renal failure). In particular, RA patients treated with MTX and IFX tend to be under immunosuppressive conditions and the utility of TST decreases.

In particular the concern of our study was that only QFT-G was able to confirm LTBI in two patients. Although caution is required when QFT-G is positive and conventional approaches are negative, it is reasonable to consider QFT-G positivity as being LTBI, as several reports have demonstrated the high sensitivity and specificity of QFT-G [6–8]. QFT-G positivity should be judged as Th1 type T cells responding *M. tuberculosis*, and thus INH prophylaxis is imperative during IFX treatment in RA patients [14]. In some cases, however, QFT-G did not present positive results where LTBI was diagnosed by conventional proce-dures. QFT-G was negative in three of five patients judged as having LTBI conventionally. These results are consistent with reports that TST has higher sensitivity than interferon γ assay for diagnosis of LTBI in old tuberculosis infection cases [15, 16]. In addition, since longer incubation periods are necessary for detection of LTBI, assay conditions may need to be adjusted in the case of RA patients treated with IFX [17].

Further examination is necessary regarding cases 2, 3, 6 and 8, as INH prophylaxis was necessary according to con-ventional procedures, while QFT-G was negative. In fact, QFT-G negativity during anti-TNF inhibitor administration does not necessarily support the absence of tuberculosis infection according to CDC recommendations [10]. There-fore, it is impossible to confirm the presence of LTBI based on the results of QFT-G alone. The results of conventional diagnostic methods (TST, imaging and medical history) and QFT-G should be used in parallel, and INH prophy-laxis should be initiated if any method gives a positive result.

It has been reported that the rate of indeterminate test results is higher for QFT-G and is associated with immuno-suppression [6]. One study in children reported a 17% rate of indeterminate QFT-G results [16]. However, only 5%

cases could not be evaluated in the present study, despite the use of IFX associated with MTX and corticosteroids. Thus, there do not seem to be any serious problems with the clinical application of QFT-G to RA patients treated with IFX and MTX.

The influence of INH on QFT-G responsiveness remains undetermined, although it has been reported that sensitivity of interferon γ assay is low in comparison with TST after treatment for active tuberculosis infection [13]. In this study, INH prophylaxis was performed in four spatients (cases 1, 2, 6 and 7). Of these patients, a decrease in QFT-G value under INH prophylaxis was observed in cases 2 and 7. These findings support the notion that administration of INH causes a decrease in QFT-G value. At present, it is uncertain whether QFT-G negativity is sufficient grounds to stop INH administration. Cases presenting positive QFT-G should thus be followed for future investigations.

Several potential limitations in this study should be considered when interpreting the results. Firstly, the study population was small and we could not perform QFT-G before the start of IFX administration in all cases. Secondly, we could not establish a study group in which no INH prophylaxis was performed despite a positive QFT-G. To confirm the utility of QFT-G in LTBI diagnosis for the purposes of preventing tuberculosis onset associated with anti-TNF inhibitor treatment, it is necessary to compare the incidence rate of tuberculosis onset among four groups classified with respect to positive or negative QFT-G before IFX and INH use or non-use. However, it is unrealistic to perform the above-mentioned comparison because of the present condition that IFX is used for RA treatment, with due consideration given to tuberculosis prophylaxis. Thus, we performed an observational study and compared QFT-G with conventional approaches for diagnosis of LTBI. Further investigations into the performance of QFT-G in those with immunosuppression are required in order to understand the better performance of QFT-G in detecting LTBI.

Conclusion

Although the advantages of QFT-G in the diagnosis of LTBI are reported to be high in specificity and sensitivity, there have been no reports regarding the utility of QFT-G in anti-TNF inhibitor treatment for RA. We performed the study focusing on the utility of LTBI monitoring by QFT-G in RA patients with IFX treatment, and the results were compared with conventional approaches (tuberculin skin test, imaging and medical history). Seven of fourteen patients were confirmed as LTBI positive by at least one method. Of these, four were positive on QFT-G during the study period, and two were positive before the start of IFX administration. The rate of agreement between QFT-G and

conventional procedures was 64.3%. A total of 5% of QFT-G tests were impossible to judge due to decreased reactions in the positive control. These results suggest that QFT-G is able to detect LTBI in RA patients overlooked by conventional methods during IFX administration. Conventional procedures and QFT-G should thus be employed in parallel, and LTBI should be assumed when one technique gives a positive result, after which prophylactic INH should be administered.

References

1. Hochberg MC, Lebwohl MG, Pelvy SE (2005) sThe benefit/risk profile of TNF-blocking agents: findings of a concensus panel. Semin Arthritis Rheum 34:819–836
2. Keane J, Gershon S, Wise RP, Mirabile-Levens E, Kasznica J, Schwieterman WD, Siegel JN, Braun MM (2001) Tuberculosis associated with infliximab, a tumor necrosis factor a-neutralizing agent. N Engl J Med 345:1098–1104
3. Gomez-Reino JJ, Carmona L, Valverde VR, Mola EM, Montero MD (2003) Treatment of rheumatoid arthritis with tumor necrosis factor inhibitors may predispose to significant increase in tuberculosis risk. Arthritis Rheum 48:2122–2127
4. Jasmer RM, Nahid P, Hopewell PC (2002) Latent tuberculosis infection. N Engl J Med 347:1860–1866
5. Tissot F, Zanetti G, Francioli P, Zellweger JP, Zysset F (2005) Influence of Bacilli Calmette-Guerin vaccination on size of tuberculin skin test reaction: to what size? Clin Infect Dis 40:211–217
6. Richeldi L (2006) An update on the diagnosis of tuberculosis infection. Am J Respir Crit Care Med : [Epub ahead of print]
7. Ferrara G, Losi M, D'Amico R, Roversi P, Piro R, Meacci M, Meccugni B, Dori IM, Andreani A, Bergamini BM, Mussini C, Rumpianesi F, Fabbri LM, Richeldi L (2006) Use in routine clinical practice of two commercial blood tests for diagnosis of infection with *Mycobacterium tuberculosis*: a prospective study. Lancet 367:1328–1334
8. Mori T, Sakatani M, Yamagishi F, Takashima T, Kawabe Y, Nagao K, Shigeto E, Harada N, Mitarai S, Okada M, Suzuki K, Inoue Y, Tsuyuguchi K, Sakaki Y, Mazurek GH, Tsuyuguchi I (2004) Specific detection of tuberculosis infection. An interferon-γ-based assay using new antigens. Am J Respir Crit Care Med 170:59–64
9. Miyasaka N, Takeuchi T, Eguchi K (2006) Guidelines for the proper use of eternercept in Japan. Mod Rheumatol 16:63–67
10. Mazurek GH, Jereb J, Lobue P, Iademarco MF, Metchock B, Vernon A (2005) Guidelines for using the QuantiFERON-TB Gold test for detecting *Mycobacterium tuberculosis* infection, United States. MMWR Recomm Rep 54:49–55
11. CDC (2005) Guidelines for the investigation of contacts of persons with infectious tuberculosis. MMWR Recomm Rep 54:1–37
12. Brock I, Weldingh K, Lillebaek T, Follmann F, Anderson P (2004) Comparison of tuberculin skin test and new specific blood test in tuberculosis contacts. Am J Respir Crit Care Med 170:65–69
13. Pai M, Riley LW, Colford MC (2004) Interferon-γ assay in the immunodiagnosis of tuberculosis: a systemic review. Lancet Infect Dis 4:761–776
14. Gardam MA, Keystone EC, Menzies R, Manners S, Skamene E, Long R, Vinh DC (2003) Anti-tumor necrosis factor agents and tuberculosis risk: mechanisms of action and clinical management. Lancet Infect Dis 3:148–155
15. Brock I, Ruhwald M, Lundgren B, Westh H, Mathiesen LR, Ravn P (2006) Latent tuberculosis in HIV positive, diagnosed by the M. Tuberculosis specific interferon gamma test. Respir Res 7:56

16. Connell TG, Curtis N, Ranganathan SC, Buttery JP (2006) Performance of a whole blood interferon gamma assay in detecting latent infection with *Mycobacterium tuberculosis* in children. Thorax 61:616–620

17. Dheda K, Udwadia ZF, Huggett JF, Johnson MA, Rook GAW (2005) Utility of the antigen-specific interferon-g assay for the management of tuberculosis. Curr Opin Pulm Med 11:195–202

−142−

Original article

Inhibitory effect of endothelin A receptor blockade on tumor growth and liver metastasis of a human gastric cancer cell line

Rika Fukui[1,3,4], Hidefumi Nishimori[1], Fumitake Hata[1,5], Takahiro Yasoshima[3,4], Keisuke Ohno[1],
Yoshiyuki Yanai[2,3,4], Kenjiro Kamiguchi[2], Ryuichi Denno[1], Noriyuki Sato[2], and Koichi Hirata[1]

[1] First Department of Surgery, Sapporo Medical University School of Medicine, South-1, West-16, Chuo-ku, Sapporo 060-8543, Japan
[2] First Department of Pathology, Sapporo Medical University School of Medicine, Sapporo, Japan
[3] Institute of Gastroenterology, Shinsapporo Keiaikai Hospital, Sapporo, Japan
[4] Department of Surgery, Shinsapporo Keiaikai Hospital, Sapporo, Japan
[5] Department of Surgery, Eniwa Daiichi Hospital, Eniwa, Japan

Abstract
Background. With metastatic progression, gastric cancer is incurable. Using a DNA microarray, we performed differential gene expression analysis of established highly metastatic gastric cancer cell lines and compared the findings with those from a low-metastatic parental cell line. The results demonstrated that the endothelin A receptor (ET-A) gene was the only one from the highly metastatic cell lines that was generally up-regulated.
Methods. To investigate the role that ET-A plays in gastric cancer metastasis, we studied the effect of an ET-A-selective antagonist, YM598, on cell proliferation, tumor growth, and liver metastasis of the highly liver metastatic cell line AZ-H5c, established from the low metastatic human gastric cancer cell line AZ-521.
Results. An in vivo study using nude mice demonstrated that YM598 had a significant growth inhibition effect on AZ-H5c at doses of 0.5–10.0 mg/kg. The liver metastatic rate was also significantly reduced by YM598: control, 83.3%; 1 mg/kg dosage, 16.7%; 10 mg/kg, 20%; and pretreatment at 1 mg/kg, 16.7%. There was no evidence of gross toxicity resulting from the YM598 treatment.
Conclusion. The ET-A blockade by YM598 had a strong inhibitory effect against tumor growth and liver metastasis of the gastric cancer cell lines. These data suggest that YM598 has potential as a novel therapeutic agent for inhibiting liver metastasis of gastric cancer.

Key words Endothelin A receptor · Gastric cancer · Liver metastasis · Metastasis-related gene · Microarray analysis

Introduction

Gastric cancer is the main cause of cancer death in Japan. In particular, more efficacious treatment modalities are needed for metastatic gastric cancer. In this

study, to determine the metastasis-related genes of gastric cancer, we analyzed the differential gene expression of established human gastric cancer cell lines — AZ-H5c, a highly liver metastatic cell line; AZ-P7a, a cell line with high peritoneal dissemination; AZ-L5G, a highly lymph node metastatic cell line — and compared the findings with those from AZ-521, a parental low metastatic cell line. The results revealed that the ET-A gene was the only one of three highly metastatic cell lines that was generally up-regulated, in contrast to the AZ-521 line. Thus, we evaluated the possibility that ET-A might play an important role in the mechanism of gastric cancer metastasis and that the ET-A blockade could have an antimetastatic effect. We conducted in vitro and in vivo experiments using a non-peptide-selective ET-A antagonist, YM598 (Astellas Pharma, Tokyo, Japan). The present study demonstrates the inhibitory effect of ET-A blockade on the cell proliferation, tumor growth, and liver metastasis of gastric cancer.

Materials and methods

Animals

Athymic female BALB/c nu/nu mice used; they were 5–7 weeks old and weighed 20–22 g. They originated from the Central Institute for Experimental Animals (Kawasaki, Japan) and were purchased from Clea Japan (Tokyo, Japan). The mice were maintained in a laminar airflow cabinet under specific pathogen-free conditions and were provided with sterile food and water. All experiments were performed according to institutional ethical guidelines on animal care.

Cell lines and cell culture

A human gastric cancer cell line, AZ-521 (obtained from the Japanese Cancer Research Resources Bank,

Tokyo, Japan), and established highly metastatic variants, AZ-H5c (a liver metastatic line), AZ-P7a (a peritoneal dissemination line), and AZ-L5G (a lymph node metastatic line), were used in this study [1–3]. These three highly metastatic variants were established in our institution as previously described [1–3]; their metastatic rates are presented in Fig. 1. The cell lines were maintained in a humidified atmosphere of 95% air and 5% CO_2 at 37°C by culturing in an RPMI 1640 medium (Asahi Techno Glass, Funabashi, Japan) supplemented with 10% fetal bovine serum (FBS) (GIBCO, Grand Island, NY, USA), tylosin tartrate 8μg/ml (Sigma-Aldrich, St. Louis, MO, USA), penicillin 50 units/ml, and streptomycin 50mg/ml (GIBCO). The cells were passaged and expanded by trypsinization of cell monolayers followed by replating every 4–5 days. The culture medium was changed every 2–3 days.

Target preparation

Differential gene expression among the four cell lines was measured. First, poly(A)⁺mRNA was extracted from cultured cell pellets using a Fast Track mRNA Isolation Kit (Invitrogen, Carlsbad, CA, USA) according to the manufacturer's instructions and quantified spectrophotometrically. Double-stranded cDNA was synthesized from purified poly(A)⁺mRNA using the T7-(dt)$_{24}$ primer (5'-GGCCAGTGAATTGTAAGTA ATACGACTCACTATAGGGAGGCGG-(dt)$_{24}$-3') and a Superscript Kit (Invitrogen). Double-stranded

cDNA was purified by phenol/chloroform extraction with phase lock gels. Biotin-labeled antisense cRNA (target) in an in vitro transcription reaction (IVT) was produced using the ENZO BioArray RNA Transcript Labeling Kit (Affymetrix, Santa Clara, CA, USA). The IVT product (cRNA) was then cleaned up using QIAGEN RNeasy Columns (Qiagen, Hilden, Germany) according to the manufacturer's instructions. Subsequently, the cRNA was fragmented for target preparation.

Target hybridization and washing, staining, and scanning probe arrays

A hybridization cocktail was prepared using a Gene Chip eukaryotic Hybridization Control Kit (Affymetrix). The cocktail was then hybridized on the Gene Chip Human Cancer G110 Array (Affymetrix) during a 16-h incubation in a 45°C oven. Before hybridization to the G110 array, the target RNA quality was determined by hybridization to the Affymetrix Test 2 Array.

Immediately following hybridization, the hybridized probe array was subjected to an automated washing and staining protocol on the fluid station according to the Gene Chip Fluidics Station 400 User's Manual. Each probe array was scanned twice. The computer workstation automatically overlaid the twice-scanned images and averaged the intensities of each probe cell for the greatest assay sensitivity.

Array data analysis

Data were analyzed using Microarray Suite 4.0 software (Affymetrix). The software calculated the average intensity of the signals from each probe array and then applied the selected array algorithm to determine the expression levels for each gene. The average expression level of each gene in each cell line was calculated, and the ratio of the average expression level between the two cell lines was then calculated. Comparative analysis of the parental cell line, metastatic cell lines, and each metastatic cell line was performed. The cutoff value was set at 3.0 for the ratio.

Detection of mRNAs by RT-PCR

Total RNA was extracted from the four cell lines with the QIAGEN RNeasy Mini Kit according to the manufacturer's instructions. All RNA samples were quantified by spectrophotometry and stored at −80°C until processed for reverse transcription (RT). First-strand cDNA was synthesized from 1μg of the total RNA using the Super Script Choice System for cDNA Synthesis in 19μl of reaction volume, according to the instructions
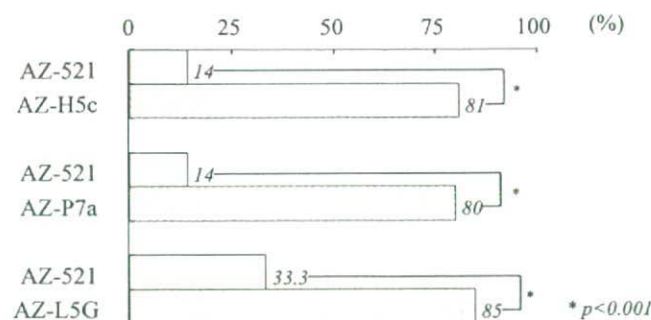

Fig. 1. To evaluate the metastatic potential, cultured cells from each cell line were inoculated into the spleen (AZ-H5c, 5×10^6 cells), peritoneal cavity (AZ-p7a, 1×10^7 cells), and perigastric wall (AZ-L5G, 5×10^6 cells) of nude mice. Three weeks after inoculation, the mice were sacrificed and examined for metastasis. The three established cell lines demonstrated significantly higher metastatic ability than the parental AZ-521 cells. The liver metastatic rate of AZ-H5c was 81%; the peritoneal dissemination rate of AZ-P7a was 80%; and the lymph node metastatic rate of AZ-L5G was 85%. In contrast, the metastatic rates of AZ-521 were 14% for the liver, 14% for the peritoneal cavity, and 33.3% for the lymph nodes. *$P < 0.001$ versus control